



**Joana Alexandra  
Assunção Mendes**

**Otimização de um sistema operacional para  
previsão de eventos extremos de maré no estuário  
de Santos (Brasil)**

**Optimization of an operational forecast system for  
extreme tidal events in Santos estuary (Brazil)**





**Joana Alexandra  
Assunção Mendes**

**Otimização de um sistema operacional para  
previsão de eventos extremos de maré no estuário  
de Santos (Brasil)**

**Optimization of an operational forecast system for  
extreme tidal events in Santos estuary (Brazil)**

*“The sea, once it casts its spell, holds one in its net of wonder  
forever”*

— Jacques Cousteau





**Joana Alexandra  
Assunção Mendes**

**Otimização de um sistema operacional para  
previsão de eventos extremos de maré no estuário  
de Santos (Brasil)**

**Optimization of an operational forecast system for  
extreme tidal events in Santos estuary (Brazil)**

Dissertação apresentada à Universidade de Aveiro para cumprimento dos requisitos necessários à obtenção do grau de Mestre em Ciências do Mar e da Atmosfera, realizada sob a orientação científica do Doutor João Miguel Dias, Professor Associado c/ Agregação do Departamento de Física da Universidade de Aveiro, e do Doutor Paulo Chambel Leitão, Investigador na Empresa Hidromod.



Dedico este trabalho aos meus pais e irmão.





**o júri**

Presidente

**Prof. Doutor José Manuel Henriques Castanheira**

Professor Auxiliar do Departamento de Física da Universidade de Aveiro

Arguente

**Doutor José Manuel Chambel Filipe Lopes Leitão**

Gerente da Hidromod - Modelação em Engenharia, Lda.

Orientador

**Prof. Doutor João Miguel Sequeira Silva Dias**

Professor Associado c/ Agregação do Departamento de Física da Universidade de Aveiro



## **agradecimentos / acknowledgements**

The conclusion of this thesis would never be possible without the scientific help and psychological support of several persons. I feel the need and the obligation to thank you all for your support and guidance considering such an intense year of constant learning and constant doubting.

Firstly, I would like to thank Prof. Dr. João Miguel Dias for his scientific supervision and valuable advices not only during the academic track but also in personal life. Your encouragement over the last years during my academic path defined the career path I would like to achieve.

To NMEC colleagues for the knowledge sharing and good times spent at the laboratory.

To HIDROMOD staff for receiving me so well. A special thanks to Dr. Paulo Leitão Chambel for his mentorship, for all the time and effort spent, for teaching me so much even when I was not believing the results. Thanks for the guidance, persistence, trust, and important insights. Also, a special thanks to Dr. José Leitão whose expertise and scientific discussions were crucial to the conducting of this thesis. I am truly grateful knowing that this was a rewarding journey.

A special thanks to Praticagem and UNISANTA for data providing.

Sofia, words cannot express my gratitude for your attention and care to me. Thanks for the suggestions and ideas during this research and for always keeping me motivated. You deserve the world.

To João Rodrigues, for the help in solving several problems, whose technical support in programming skills and valuable suggestions were crucial, especially in the numerical model setup. Thank you!

To Diana, Mara, Nicole, and Pedro, for making these graduation years the time of my life. Thanks for our frustrations and conquers sharing. I feel this was never an individual path, but a route we conquered together. I still cannot believe how I was able to continue this without you. You are the true meaning of college friends are for life even when living in continents apart.

To Rui, who has no idea how important his support was for me, always keeping me motivated to work hard and learn with failures. Thanks for being always there during the conducting of this master. My most sincere gratitude to Filipa, for your friendship, support, and for always being able to listen to me.

To my parents, that cried rivers when first left me in Aveiro. Thanks for your unconditional support who was essential during this course. Thanks for never discourage me in my very own curiosity to go out and explore the world. Thanks for always being the port and for guiding me on the right path. Thanks for letting me grow freely, knowing the roots. Your love, understanding and support make my life meaningful. This is mainly dedicated to you.

To Bernardo for the support and comprehension.

Thank you all for your continued support, enthusiasm, dedication and passion you've given me. To you all I owe the achievement of this thesis.



## Palavras Chave

Estuário de Santos, Hidrodinâmica, Modelação Numérica, Oceanografia Operacional, Condições Fronteira.

## Resumo

Atualmente, a previsão da circulação estuarina é um tópico de grande importância, especialmente em regiões com elevada densidade populacional, como é o caso da região de Santos. O presente trabalho pretende otimizar a qualidade da previsão do nível de água no estuário de Santos, particularmente os forçamentos físicos que determinam as marés residuais. Em casos extremos, os níveis de água observados e previstos podem diferir significativamente, aumentando os erros de previsão, revelando a importância da compreensão destes fenómenos, para proposta de medidas corretivas. Estes eventos têm consequências tanto para as atividades de navegação portuária, como para as populações que habitam nas zonas marginais ao estuário. A presente dissertação analisa dados observados do nível de água e altura significativa da onda, para o período de 2016 a 2017. Os dados utilizados foram registados em 5 estações e foram cedidos pelos Pilotos da Barra e Praticagem. Foi utilizado o modelo hidrodinâmico MOHID 2D ([www.mohid.com](http://www.mohid.com)), usando um método de "downscaling", conectado ao software AQUASAFE que fornece previsões de alta resolução para auxílio em tempo-real à navegação. O modelo foi validado para o período de 2016-2017, sendo que os valores mínimos RMSE foram de 12.5 cm e praticamente todas as estações apresentaram um SKILL excelente. Foi implementada a mais recente solução global astronómica (FES2014) como condição de fronteira oceânica. Adicionalmente, foi alterada a implementação da condição fronteira oceânica meteorológica (CMEMS) de dados diários para horários. Foi ainda estudada a possível influência da altura significativa da onda na previsão do nível de água (particularmente na maré residual). Devido à grande correlação encontrada entre ambos os parâmetros, foi desenvolvida uma metodologia de regressão linear para correção em pós-processamento da maré residual para determinadas condições de agitação marítima. A aplicação de diferentes condições fronteira nos modelos preditivos (meteorológico e astronómico) diminuiu os erros das previsões numéricas, o que claramente melhorou a capacidade preditiva dos modelos. No entanto, a aplicação da solução FES2014 apesar de reduzir os erros na embocadura do estuário, conduz ao seu aumento nas zonas interiores. Este resultado indica a necessidade da obtenção de novos dados batimétricos, considerando que os erros na componente astronómica de maré aumentam em direção à cabeceira do estuário. Os erros da maré residual mantêm-se praticamente inalteráveis ao longo das estações, sendo superiores em situações de tempestade. Os resultados evidenciam que as modificações do modelo melhoram a precisão na reprodução do nível de água, comparando com a versão anterior, particularmente no caso de ocorrência de eventos extremos.



## Keywords

Santos Estuary, Hydrodynamic, Numerical Modelling, Operational Oceanography, Boundary Conditions.

## Abstract

Forecasting estuarine circulation is in high demand, especially in regions of high population density like Santos region. Present work intends to optimize the performance of the water level forecast for Santos Estuary, particularly, the physical forcing determining the residual tide. In extreme cases, predicted and observed water level can significantly differ, increasing significantly the predicting errors, which highlights the need to understand the factors that affect the residual tide to propose corrective measures. Furthermore, the extreme events have potentially hazardous consequences not only for navigation purposes, as also to the population that live nearby the channels. This dissertation analyzes the water level and significant wave height dataset covering the period of 2016 to 2017. Datasets comprehend 5 tide gauge stations in Santos channel and were obtained from the Pilotos da Barra and Praticagem. MOHID 2D hydrodynamic model ([www.mohid.com](http://www.mohid.com)) was used, implemented with a nested downscaling approach, being linked to AQUASAFE software that provides high-resolution forecast to give support to navigation in real-time. The model was validated for the period of 2016-2017, being minimum RMSE found of 12.5 cm and practically all stations present an excellent SKILL. The most recent astronomical global solution (FES2014) was implemented as oceanic boundary condition. Additionally, the meteorological boundary condition (CMEMS) was altered from daily to hourly data. It was also researched the possible influence of wave height on the forecast of water level (particularly the residual tide). Due to the great correlation found among these parameters, a linear regression method was developed to correct in post-processing stage the residual tide under specific wave height conditions. The appliance of distinct boundary conditions on forecasting models (meteorological and astronomical) decreased errors when compared to observations, evidencing the improvement of forecast capacity. On the other hand, the use of FES2014 shows improvements at the bay entrance, however, results get worst in the inner stations. This portrays the need of reliable bathymetric data due to increasing errors on the astronomical tidal components towards the end of the estuary. Residual tide errors remain practically constant along the estuary, however, they increase under extreme conditions. The results evidence that model modifications improve the accuracy in reproducing the water level evolution, comparing to the previous version, particularly under extreme events.





# Contents

Contents	xvii
List of Figures	xix
List of Tables	xxi
Nomenclature	xxii
<b>1 Introduction</b>	<b>1</b>
1.1 Motivation and aims . . . . .	1
1.2 State of the art . . . . .	4
1.3 Structure of this work . . . . .	6
<b>2 Study area</b>	<b>7</b>
2.1 General description . . . . .	7
2.2 Physical description . . . . .	8
2.2.1 Wind regime . . . . .	8
2.2.2 Precipitation . . . . .	9
2.2.3 Freshwater discharge . . . . .	11
2.2.4 Sea level: astronomical tide . . . . .	11
2.2.5 Sea level: meteorological tide . . . . .	13
2.2.6 Currents . . . . .	13
2.2.7 Wave regime . . . . .	15
2.2.8 Water temperature and salinity regime . . . . .	15
<b>3 The numerical model: MOHID2D</b>	<b>17</b>
3.1 Governing equations . . . . .	17
3.2 Numerical grids . . . . .	18
3.3 Boundary conditions . . . . .	20
3.4 Validation . . . . .	20

<b>4</b>	<b>Data and Methodology</b>	<b>22</b>
4.1	Sea level and wave data . . . . .	22
4.2	Sea level components decomposition . . . . .	23
4.2.1	Bias . . . . .	23
4.2.2	Astronomical tide . . . . .	24
4.2.3	Residual tide . . . . .	25
4.2.4	Statistical analysis of water level . . . . .	26
4.3	FES2014 implementation . . . . .	27
4.4	CMEMS implementation . . . . .	28
4.5	Post-processing correction method . . . . .	29
<b>5</b>	<b>Results and discussion</b>	<b>30</b>
5.1	Numerical model validation . . . . .	30
5.2	Astronomical tide assessment . . . . .	33
5.2.1	Harmonic analysis . . . . .	33
5.2.2	HC and RHC . . . . .	36
5.3	Tidal propagation characterization . . . . .	37
5.4	Boundary conditions assessment: FES2014 . . . . .	41
5.5	Residual tide assessment . . . . .	43
5.5.1	Boundary conditions assessment: CMEMS . . . . .	43
5.5.2	Investigating residual tide errors . . . . .	44
<b>6</b>	<b>Conclusion</b>	<b>55</b>
	<b>References</b>	<b>58</b>

## List of Figures

1	Map of the study area with the location of the Port of Santos . . . . .	7
2	Orography of Santos region . . . . .	9
3	Normal monthly mean values of sea level pressure, air temperature, surface winds . . . . .	10
4	Normal monthly mean values of precipitation and evaporation . . . . .	10
5	Map of coastal area of Santos bay with main freshwater tributaries . .	11
6	Overlap of $M_2$ , $M_3$ , and $M_4$ tidal components . . . . .	12
7	Surface and depth mean currents based on measurements at several depths	14
8	Vertical profiles of water temperature and salinity representing winter conditions during flood-spring-tide conditions . . . . .	15
9	Vertical profiles of physical properties temperature and salinity repre- senting summer conditions during flood-spring-tide conditions . . . . .	16
10	Hydrodynamic numerical grids and bathymetry . . . . .	18
11	Location of the 5 tide gauges along Santos estuary . . . . .	22
12	Reduced level for the 5 tide gauges along Santos estuary . . . . .	23
13	Comparison between predicted and observed mean sea level for the 5 tide gauges along Santos estuary . . . . .	30
14	Taylor diagrams for the 5 tide gauges along Santos estuary . . . . .	32
15	Harmonic constants (amplitude and phase) determined from model pre- dictions and observations . . . . .	35
16	<i>HC</i> and <i>RHC</i> error for the 5 tide gauges in Santos estuary . . . . .	37
17	Distribution of $M_2$ and $S_2$ amplitude and phase for Santos estuary . . .	39
18	Distribution of $M_3$ and $M_4$ amplitude and phase for Santos estuary . .	40
19	<i>HC</i> and <i>RHC</i> error for the 5 tide gauges in Santos estuary with the new implementation . . . . .	42
20	Residual tide observed and daily and hourly CMEMS resolution . . . .	45
21	Comparison between observed significant wave height and residual tide determined for S1 station . . . . .	46
22	Significant wave height data observed . . . . .	48

23	Linear regression between $H_s$ and residual error . . . . .	49
24	Indexes of $H_s$ , model, model correction and observations of residual tide	51
25	Comparison between observed residual and computed residual for a storm event . . . . .	52
26	Indexes of $H_s$ for model, model correction and observation of residual tide	54

## List of Tables

1	Tidal current velocities in Santos estuary . . . . .	14
2	Summary of hydrodynamic model for Santos estuary application . . . .	19
3	Global and region numerical modeling network. . . . .	21
4	Tidal gauges along Santos estuary . . . . .	22
5	Main harmonic constituents description . . . . .	25
6	Statistical parameters for water level for the 5 tide gauges in Santos estuary . . . . .	30
7	Statistical parameters for astronomical tide for the 5 tide gauges in Santos estuary . . . . .	33
8	Harmonic constituents amplitude and phase for all stations in Santos estuary . . . . .	34
9	Form factor determined from observations and predictions for Santos estuary . . . . .	38
10	Sum of the amplitudes and relative importance of the main tidal constituents . . . . .	38
11	Harmonic constituents amplitude and phase differences for the 5 tide gauges in Santos estuary for FES2012 and FES2014 solutions . . . . .	41
12	Statistical parameters for residual tide for the 5 tide gauges in Santos estuary . . . . .	43
13	Residual tide comparison between observations and daily and hourly CMEMS results . . . . .	44
14	Correlation coefficient between residual tide and $H_s$ . . . . .	47
15	Statistical analysis of residual tide for total time series and for $H_s$ higher than 1.5 m . . . . .	47
16	Maximum residual tide for extreme events of maximum value of $H_s$ and respective residual error . . . . .	49
17	Statistical analysis of residual tide for $H_s$ higher than 1.5 m with and without correction factor . . . . .	50
18	Statistical analysis of residual tide for $H_s$ higher than 1.5 m with and without correction factor . . . . .	53



# Nomenclature

CLS Collecte Localisation Satellites

CMEMS Copernicus Marine Environment Monitoring Service

CNES National Centre for Space Studies

COFS Coastal Ocean Forecasting Systems

DHN Diretoria de Hidrografia e Navegação

FES2012 Finite Element Solution 2012

FES2014 Finite Element Solution 2014

GFS Global Forecast System

HC Mean Complex Amplitude Error

INPH Instituto Nacional de Pesquisas Hidroviárias

IST Instituto Superior Técnico

IWA International Water Association

LEGOS Laboratoire d'Etudes en Géophysique et Océanographie Spatiales

MOHID Water Modelling System

NCAR National Center for Atmospheric Research

NCEP National Center for Environmental Prediction

NE Northeast

NOAA National Oceanic and Atmospheric Administration

NPH-UNISANTA Núcleo Pesquisas Hidrodinâmicas - Universidade de Santa Cecília

NW Northwest

RHC Relative Mean Complex Amplitude Error

SIGRH Sistema Integrado de Gerenciamento de Recursos Hídricos do Estado de São Paulo

# 1 Introduction

The present section will expose the motivation and need to perform this research as well as the main purpose and sub objectives. Also, a literature review on the main research for the present study region are comprehensibly reviewed.

## 1.1 Motivation and aims

Estuarine systems are extremely dynamic in time and space, and can be found in coastal areas around the world. They are characterized as transitional environments, connecting freshwater, marine and terrestrial environments, from where they receive a huge amount of nutrients and organic matter.

From a human historic perspective, the intrinsic characteristics of estuaries have made them preferable sites of occupation and, consequently, intense areas of development. A direct consequence of the human occupation of these coastal areas is that estuaries rank among the environments most affected by the human presence and their activity (Mateus et al., 2008).

The Santos estuary, located in Brazil, is a very important estuarine system, which main socio-economic drivers are the industrial and port activities. Also, the Port of Santos, the most important harbor of Latin America, plays a significant role for the brazilian and international economy. Cubatão city (north of Santos estuary) has a relevant industrial pole with different kinds of industries, but mainly associated with the petroleum products, fertilizer production and a very important steel production (Mateus et al., 2008). Therefore, not only Santos estuary endures great urban pressure regarding the large population that live nearby its margins, but also the activities enrolled in this area turning it into a polluted area.

In recent years, there has been a growing concern to maintain a steady growth in economic activities and social development in estuarine areas, while preserving their natural features and ecological services (Mateus et al., 2008).

Therefore, there is major interest in understanding the physical processes that dominate the estuary, in order to support effective decision-making regarding specific coastal activities. Several areas are entirely dependent on the knowledge of the estuaries dynamics, such as coastal engineering, fisheries, marine environment, and oceanography.



The Santos estuary is both ecologically and economically very important, deserving, therefore, special attention in terms of scientific research.

Nowadays, there is increasing interest in implementing predictive estuarine hydrodynamic models, since they are key tools to study the main local processes of estuarine areas. Observational programs often do not cover entire study areas, therefore estuarine hydrodynamic models may be used to complement observations (Vaz and Dias, 2013). Moreover, due to human and material limitation, it is often difficult to have enough information provided by field measurements, thus numerical models appear to be the better alternative in these cases. This demonstrates the importance of the set-up of numerical models in improving estuarine and coastal dynamics understanding.

The accuracy of tidal models in predicting the coastal area hydrodynamics has been improving over the last years. Increases in computational resources have allowed the development of more robust mixing routines, higher-resolution domains, and inclusion of detailed circulation processes. Numerical modeling has emerged over the last several decades as a widely accepted tool for investigations in environmental sciences (Ganju et al., 2016).

Growing knowledge of estuarine systems implies constant development of better tools to improve and support natural events forecast. Monitoring sea level and wave data comprehends different applications such as: control of the national leveling system, oceanographic studies, climate change impacts assessment, operational purpose, harbor operations, navigation, etc.

On the other hand, many factors contribute to uncertainties in coastal ocean model forecasts. These may include: imperfect atmospheric forcing fields; errors in boundary conditions propagating inside the finer scale model domain; bathymetric errors; insufficient horizontal and vertical resolution; numerical noise; bias; errors in parameterizations of atmosphere-ocean interactions and sub-grid turbulence, etc (Kourafalou et al., 2015). Regarding shallow waters, errors remain either because of estuarine physical complexity (e.g. bathymetry) or lack of *in-situ* measurements.

It should be also pointed out the extreme importance of operational oceanography to support decision-making of ports, shipping procedures as well as scientific research. Currently, HIDROMOD together with UNISANTA is responsible for managing a forecast system - AQUASAFE (waves, sea level, currents, water quality), used to support, in real time, harbor, civil protection and water quality monitoring activities for the Santos Estuary.

The variability of water level and wave climate in the Santos estuary, specifically in extreme conditions, prevents a wide range of uses such as commercial and recreative

navigation, drainage and urban floods, which then affect the local beach water quality. Overtime, particularly in Santos system, an effort has been made to decrease prediction errors, such as sea level forecast service provided by AQUASAFE. These efforts are summed up in the several reports, covering semi-annual periods since 2015. Since then, several improvements were achieved, and continuous validation of data allows a permanent progress of forecasting systems in line with science advances.

The ensemble factors that affect the hydrodynamic (tides, meteorology, freshwater discharges) remains a challenging task particularly in terms of improving the forecast capacity of the models. Particularly, the complex sea level regime induces great difficulties for local tide predictions for the Santos estuary. In extreme cases, with the occurrence of storm surges, predicted and observed sea level can differ significantly in height, strongly increasing the errors related to tide prediction, being this a limitation of forecasting models. This strongly affects shipping procedures and navigation, causing economic loss, as may also origin floods to populations.

Therefore, the previously stated highlights the motivation and need to fully address the main physical factors that influence the hydrodynamic of Santos estuary. The present work was developed in cooperation with HIDROMOD, with the main objective of improving the forecast capacity of predicting models currently in use in the operational service AQUASAFE particularly under extreme events. Also, an effort enhancing the oceanic boundary models in the current model implementation was conducted. The relationship among physical variables to study their influence on the residual tide was studied. This led to propose a correction method in the forecasting models, not only to diminish the risks regarding all the uses and entities enrolled, but also to achieve an adequate management regarding the study area. The sub-goals of the present work include:

- Validate water level predictions for the period of 2016-2017;
- Statistical analysis of model predictions and tide gauge data for the period of 2016-2017;
- Characterize hydrodynamic patterns at Santos estuary;
- Update the current global astronomical solution in use (FES2012) to the newest version (FES2014) and validate this experiment;
- Study the appliance of a distinct temporal resolution on the oceanic boundary condition (CMEMS);

- Analysis of wave data for the period of 2016-2017;
- Investigate the correlation between wave data and physical parameters;
- Propose a correction method for the residual tide based on wave data.

Overall, this work also promotes on-going research that it is already conducted by HIDROMOD and UNISANTA to improve the knowledge of estuarine systems, particularly the navigation within the Santos estuary.

## 1.2 State of the art

The Santos estuary is a very complex system that deserves special attention in terms of scientific research to manage reasonably all its uses. Therefore, the interest in the estuary, lead to the development of several types of research in distinct scientific domains. Along with scientific and technical projects, several numerical models have been applied to represent the hydrodynamics of this coastal area, regarding a wide range of applications, such as to support navigation security, water quality monitoring, to study the impacts of dredging operations as well as sediment transport patterns. On the other hand, some physical aspects have not been addressed yet such as problems related to residual tides.

A pioneering study on the numerical modeling of the Santos estuary and the inner continental shelf forced by the main tidal components was published by Harari and Camargo (1998). Although only barotropic conditions were considered, it allowed to find out interesting features: stronger ebbing circulation east side of the bay and convergent circulation due to flooding currents in the channels of S.Vicente and Bertioga; this work was further improved by Harari and Gordon (2001) and Harari et al. (2002) with theoretical simulations of the barotropic circulation in the Piaçaguera channel, which were validated with observational results.

First MOHID implementations were assessed by Berzin et al. (1997) and Berzin et al. (1999) in a restricted area of Baixada Santista, including the estuarine area of Santos, for tidal effect simulation. These works were improved by Leitão et al. (2000), which implemented a nested grid scheme in order to simulate currents wind driven in a regional scale, as also imposed realistic boundary conditions in the local model. The Lagrangian model was applied to study sediments transport from dredged material resulting from Port of Santos dredging activities, in local model. Afterward, Leitão et al. (2005) implemented a methodology that improved the hydrodynamic validation process in MOHID for studying the coastal zone of Santos estuary. This study considered

the overlapping, in the open boundary, of the sub-inertial oscillations added linearly to the tide. It was found out that a strong correlation exists between the measured water level and the alongshore velocity component, averaged in depth. Consequently, this study illustrated the importance of considering the sub-inertial oscillations in the final solution, that clearly enhanced the hydrodynamic results.

Harari et al. (2008) intended to provide an integrated management approach to several estuarine systems in South America, including Santos estuary. In a holistic way, this approached climatology and hydrography, biogeochemical parameters as well identified socio-economic issues in Santos estuary. This project emphasized the inevitable management challenge in this area.

Campos et al. (2010) aimed to identify the synoptic scale atmospheric influence over the ocean for the occurrence of extreme sea level in Santos. Time series of water level at the Port of Santos, as well as wind and surface pressure from the NCEP reanalysis, were used over the period 1952 to 1990. Results have shown a seasonal variability, with positive extreme events occurring mainly during autumn (40.2%) and winter (30.8%), characterized by surge elevations larger than 0.38 m that depend on low-pressure systems development with southwesterly winds together with a continental anticyclone presence.

Lopes (2015) investigated the impact of deepening the Santos navigation channel on tidal asymmetries, and found a reduction of up to 20% in the ebb peak velocities during spring tide along the Santos estuary, related to the modification of relative phase of  $M_2$  and  $M_4$  in tidal currents. Moreover, an increase in diurnal inequalities of the ebb velocities, related to the periodical distortions produced by the third-diurnal tidal constituents was observed.

The applicability of a numerical model following a downscaling methodology was evaluated for the south-eastern Brazilian shelf (regional model) and Paranaguá estuarine system (local model) by Franz et al. (2016). The inclusion of  $M_3$  constituent in hydrodynamic studies in Paranaguá system appeared to be of extreme importance in terms of improving of tidal potential. Furthermore, this numerical model was developed within a operational modeling perspective, useful for navigation and emergency response such as oil spills simulation.

Advancing of Coastal Ocean Forecasting Systems (COFS), addressed by Kourafalou et al. (2015), requires the support of continuous scientific progress addressing: the primary mechanisms driving coastal circulation; methods to achieve fully integrated coastal systems (observations and models), that are dynamically embedded in larger scale systems; and methods to adequately represent air-sea and biophysical interac-

tions. Issues of downscaling, data assimilation, atmosphere-wave-ocean couplings and ecosystem dynamics in the coastal ocean are discussed. These scientific topics are fundamental for the success of COFS, and are connected to evolving downstream applications, dictated by the socioeconomic needs of rapidly increasing coastal populations. It was concluded the expected society benefits that COFS can provide while targeting user needs.

Braga et al. (2016) describes the present setup of the numerical models and observational systems used at Santos region, according to COFS concept, focusing on the system characteristics, validation of high-resolution models, and on the uncertainties detected. The AQUASAFE platform ([www.aquasafeonline.net](http://www.aquasafeonline.net)), developed by HIDROMOD, and distinguished by IWA, was used. This work details the external sources of local data collected on stations in Port of Santos connected to AQUASAFE as also the external numerical models associated. Important insights for the present work rely on the oceanic boundary conditions that are FES2012 as global astronomical solution whilst CMEMS solution for meteorological tide (in a daily temporal resolution). Model reproduces water level with linear correlation of at least 90%. However, during the occurrence of storm events associated with strong winds and high waves (e.g. significant height up to 4 meters) predictions are not so accurate, which restricts the shipping procedures in Port of Santos. Authors emphasize the continuous need for forecast improvement in line with science advance.

### **1.3 Structure of this work**

The present study is organized in the following order: the present chapter introduces the motivation and aims of this work, including important hydrodynamic studies performed in Santos estuary. The second chapter comprises a portrayal of the study area, regarding the available literature, consisting in characterizing physical aspects of Santos estuary focusing on the hydrodynamic characteristics. This includes the gathering of available data of the dominant variables in estuary dynamics. Chapter 3 includes a detailed description regarding the methods applied in this work. An overview regarding the main capabilities of the numerical model (MOHID) is given, as well as detailed information about model configuration for the present study in chapter 4. Data of tide gauges and modeling results are presented and discussed in chapter 5. Finally, chapter 6 summarizes the main final remarks and enunciates future research suggestions.

## 2 Study area

This section addresses the main physical and hydrological parameters of Santos estuary, such as: wind regime, precipitation, freshwater discharge, sea level (astronomical and meteorological), currents, wave regime, water temperature and salinity regime.

### 2.1 General description

The Santos estuary (Figure 1) is located in southeastern Brazilian coastal area ( $23^{\circ}30' - 24^{\circ}S - 46^{\circ}05' - 46^{\circ}30'W$ ), comprehending a  $835 \text{ km}^2$  basin area (Mancuso et al., 2014). The estuarine system of Santos comprises three major channels, namely S.Vicente, Santos, and Bertioga, interconnected in its inner area. Santos and S.Vicente channels comprise an approximate area of  $44.100 \text{ m}^2$ , with an average depth of 15 m in the central dredged channel of Santos and 8 m in S.Vicente channel (Mateus et al., 2008).

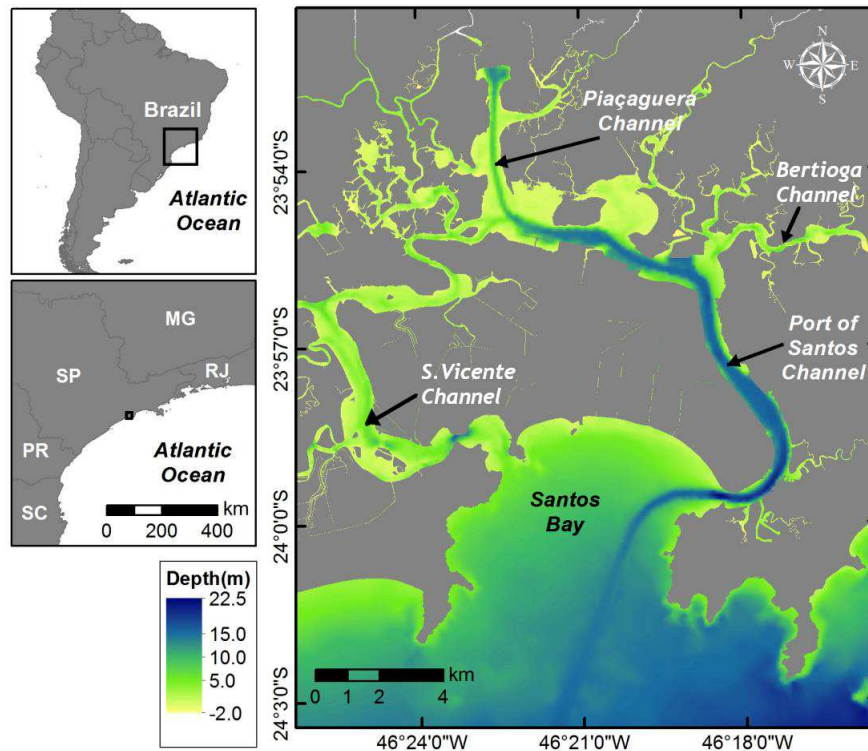


Figure 1: Map of the study area with the location of the Port of Santos. The colors indicate the local depth in meters. Adapted from: Braga et al. (2016).

The estuarine system is characterized by a flat area surrounded by scarps of the plateau of Serra do Mar (Mateus et al., 2008), being bordered by the cities of Santos, S.

Vicente, Guarujá, Bertioga and Cubatão, which is one the most industrialized of South America (Miranda et al., 2012). The coastal plains were originally covered by extensive mangrove forests, which were gradually occupied by the industrial complex of Cubatão, established since 1940, by an urban area and by the Santos harbor (Leitão et al., 2015). The development of the city has drastically modified the environmental and hydrodynamic characteristics of the estuary.

The Santos estuary can be classified as a typical sub-tropical mangrove system under significant anthropogenic pressure. The estuarine system has a considerable ecological importance, as it has a natural high productivity, being a natural habitat for many animals, like birds, mammals, fish and numerous kinds of invertebrates (Mateus et al., 2008).

Santos harbor is the most important port in Brazil, being the largest harbor in Latin America, which in 2016 traded over 114 million tons of cargo ([www.portodesantos.com.br](http://www.portodesantos.com.br)) corresponding to 10% of the total throughput of Brazil.

Santos estuary is a complex system whose geometry and river discharge have been drastically altered during the last century by urban and industrial development, land reclamation, dredging and effluent receptor from several industries (Miranda et al., 2012). Also, it is regarded as a polluted area (de Sousa et al., 1998), being heavily occupied by urban, industrial and port activities (Mateus et al., 2008).

## **2.2 Physical description**

A good physical oceanographic description of this area is fundamental to perform this research, as well as to identify the main forcings of the estuarine dynamics. The hydrodynamics and mixing processes of the Santos estuary play a key role in the transport of properties' concentration, pollutants and in the erosion, transport, and deposition of river sediments. These processes are driven mainly by the estuarine circulation (Miranda et al., 2012) and will be fully described in the following section based on present literature.

### **2.2.1 Wind regime**

The atmospheric circulation at the surface depends on the sub-tropical high-pressure center of the south Atlantic and its interactions with the sub-polar low pressures (Moscati et al., 2000); considering typical conditions, winds from the East are dominant all the seasons, with average velocities of 1.5 m/s (Harari et al., 2008). Additionally,

the complex configuration of the Santos region orography (Figure 2) strongly influences the wind regime of the Santos estuary.

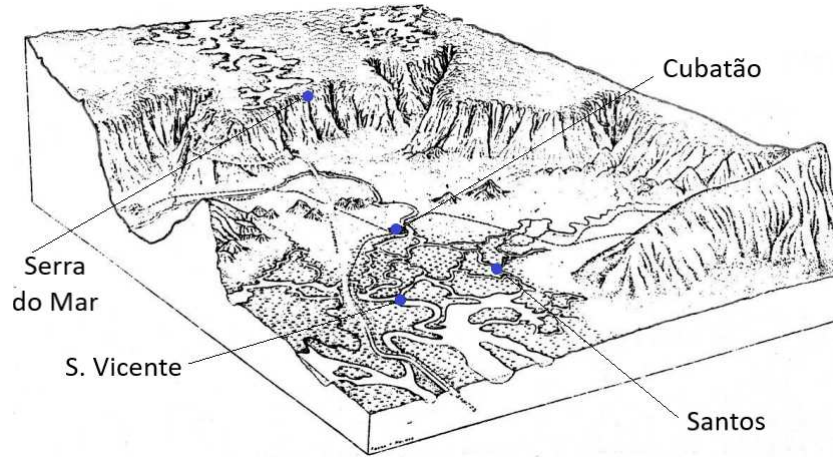


Figure 2: Orography of Santos region. Adapted from: Titarelli (1986).

However, when strong western winds occur in the limit of sub-tropical and sub-polar regions, in the Brazilian southeastern area, cold fronts modify the atmospheric conditions in the Santos estuary. Consequently, the eastern winds rotate to north and west, with atmospheric pressure falling 10 hPa (Figure 3), phenomena that take a few hours, producing strong wind intensities up to 10 m/s. This rotation is followed by winds blowing from the south for 1 to 3 days, with velocities between 5 and 10 m/s, with the decrease of air temperature and the rise of atmospheric pressure. Consequently, winds turn east again and the air temperature and pressure increase to regular values. The influence of cold fronts can be observed in Figure 3, namely a shift of the winds to NW, especially during August to October.

### 2.2.2 Precipitation

The tropical and subtropical climate causes high rainfall during summer (Harari et al., 2008), with annual precipitation between 2.000 to 2.500 mm. The estuary drains considerably large volumes of rainfall, on average 60 m<sup>3</sup>/s (FRF, 2008). The rates of precipitation and evaporation also display large annual variations (Harari et al., 2008) portrayed in Figure 4, reaching a summer peak rainfall, (December to March).

Precipitation predictions agree fairly well with data from the rain gauge stations on the coast; for example, the annual mean given by NCEP/NCAR (National Center for Atmospheric Research) is  $0.55 \pm 0.96 \text{ e-}07 \text{ m/s}$ , which corresponds to  $1734.45 \pm 3027.50$



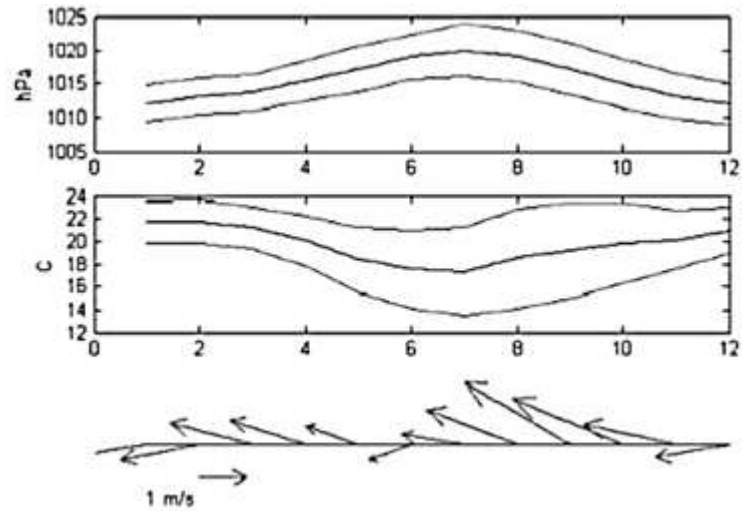


Figure 3: Normal monthly mean values of sea level pressure, air temperature, surface winds (upper to lower), as computed from NCEP / NCAR data for the period 1980 - 2004, at the position 22°30'S 45°W. Source: Harari et al. (2008)

mm/yr, while the rain gauge located at Guarujá (24°00' S 46°17'W), measured 2131.22 mm/yr (SIGRH (Sistema Integrado de Gerenciamento de Recursos Hídricos do Estado de São Paulo) - DAEE site, access in 2006 - <http://www.sigrh.sp.gov.br>) (Harari et al., 2008). The proximity of the estuary to Serra do Mar, associated with cold fronts, is responsible for the high rainfall indices in this region.

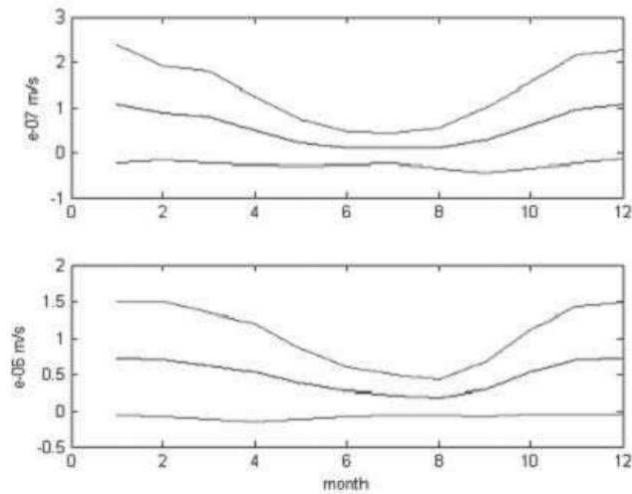


Figure 4: Normal monthly mean values of precipitation (top) and evaporation (bottom), as computed by NCEP / NCAR data for the period 1980 - 2004, at the position 22°30'S 45°W. Source: Harari et al. (2008).

### 2.2.3 Freshwater discharge

The estuary receives freshwater inflow from several small rivers that develop on the slopes of Serra do Mar, at heights of 700 m (Chambel and Mateus, 2008). The processes of erosion and transport carry high concentration of suspended matter, which is deposited in the mangrove forest and the in the estuary bed (Miranda et al., 2012). There are also many tributaries and artificial channels that collect rain drainage water and clandestine domestic waste (Mateus et al., 2008).

Therefore, six main rivers discharge in Santos estuary (Figure 5), namely a discharge of rivers Cubatão effluent which is the major freshwater contributor, river Moji and Piaçaguera that discharge together, Quilombo, Jurubatuba and Borturoca. These rivers regime have average flows of approximately  $10 \text{ m}^3/\text{s}$ .

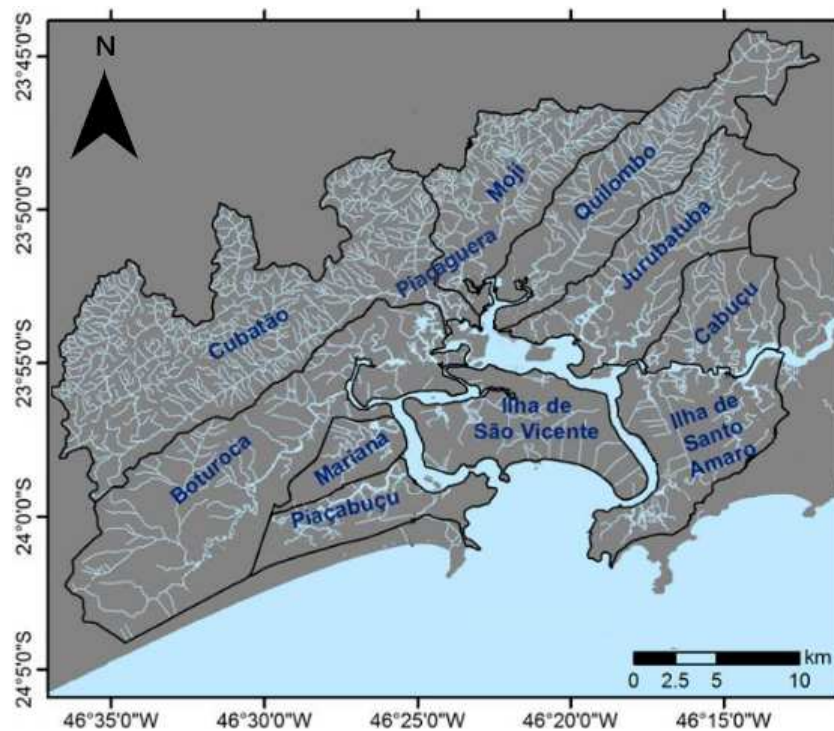


Figure 5: Map of coastal area of Santos bay with main freshwater tributaries. Adapted from: Leitão et al. (2015).

### 2.2.4 Sea level: astronomical tide

The main forcing agent driving water circulation in Santos estuary is the tide, which has an average amplitude of 1.43 m (Santos port). Thus, Santos estuary can be considered a micro-tidal estuary (ranges lower than 2 m). The estuary is partially mixed to stratified, where the salt transport within the estuary is due to the up-estuary propagation of the

salt wedge and eddy diffusion (Miranda et al., 2012), inducing changes in circulation patterns.

Pickard and Pond (1978) introduced the tidal form factor ( $F$ ) to evaluate the dominance of diurnal and semi-diurnal components. In Santos estuary,  $F$  is equal to 0.3, which corresponds to a semi-diurnal tide with daily inequalities, considering tidal astronomical components measured at Port of Santos (Speranzini, 2017). Prominent peaks occur at diurnal ( $K_1$ ,  $O_1$ ), semi-diurnal ( $M_2$ ,  $S_2$ ,  $K_2$ ), quarter-diurnal ( $M_4$ ) and lunar third-diurnal ( $M_3$ ) constituents. Smaller peaks also appear at the  $M_6$  tidal harmonic (Miranda et al., 2012). In general, all the components are amplified through the estuary. According to Lopes (2015), the  $M_2$  and  $S_2$  component amplifies utmost at the end of Piaçaguera channel: 30.6 % and 21.9 % respectively.

The south-eastern Brazilian shelf is known for the resonance of the third-diurnal principal lunar tidal constituent  $M_3$  (period of 8.28 h), related to the asymmetries in the tidal currents. The massive amplification of this constituent was firstly described by Huthnance (1980), being the largest amplitudes found in the Paranaguá estuarine system (Franz et al., 2016).

Distortions are found in every two tidal cycles, indicating that the  $M_3$  component is related to the daily inequalities in the tidal amplitudes (Lopes., 2015). In Figure 6 it is possible to observe the influence of the third-diurnal component on the tidal signal. Numbers 1 and 3 present changes in the water levels amplitude, whereas numbers 2 and 4 portray the distortion in the rise and fall periods of the water levels (Speranzini, 2017).

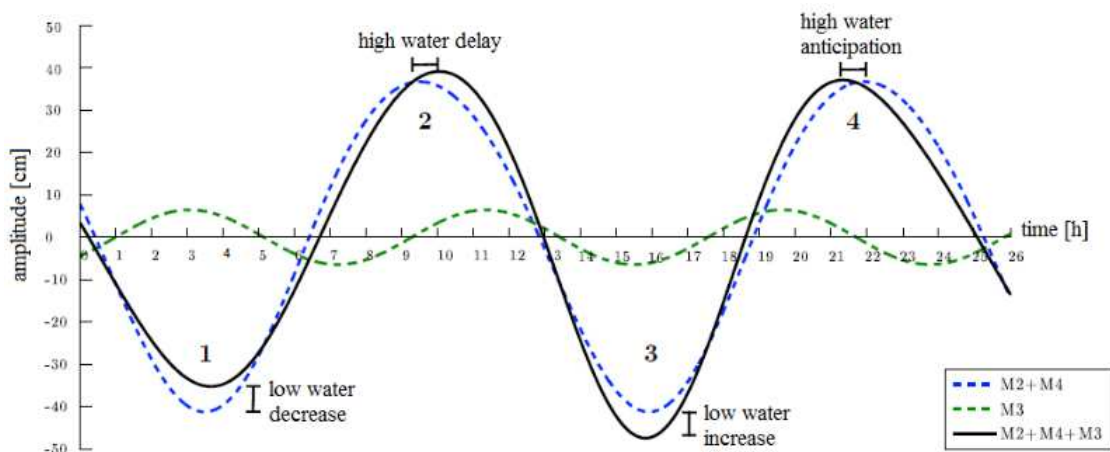


Figure 6: Overlap of  $M_2$ ,  $M_3$ , and  $M_4$  tidal components, showing the influence of the  $M_3$  in the tidal distortion. Adapted from: Lopes. (2015); Speranzini (2017).

Therefore, in the absence of meteorological significant effects, the circulation due to

astronomical tide is the principal forcing for the circulation patterns observed in Santos estuary (Harari and Camargo, 1995, 1998, 1999; Harari and Gordon, 2001).

### **2.2.5 Sea level: meteorological tide**

Apart from the astronomical tide, meteorological tide also provide significant changes in the water levels of the region. Pressure systems may rise or lower the sea level height, depending on the type of the prevailing system. Low pressure systems elevate sea levels, whereas high pressure systems tend to depress it, as a result of the inverted barometric effect. The larger water level variations are induced by low-pressure systems over the ocean. In south Brazil, these events are followed by south and south-east storms that arise mostly during autumn and winter periods. Considering the Coriolis effect on the ocean currents and the orientation of the coastline in Santos, south winds pile up the water against the coast (set-up), while north winds have the opposite effect (set-down). Transverse winds are of minor influence in the water levels of the area (Truccolo, 1998). An annual average of 12 positive extreme events of sea level were counted in the analysis of Campos et al. (2010), associated with southwesterly wind velocities above 8 m/s over the ocean, together with a continental anticyclone presence. These events are highly energetic in the estuary of Santos and are related to coastal erosion and flooding in adjacent areas (Campos et al., 2010; FAPESP, 2015; Lopes, 2015). Cold fronts (often during winter) influence water level changes that may exceed 0.5 m (Harari and Camargo, 1990; Moser et al., 2002).

According to Mancuso et al. (2014), continental shelf waves can be one of the mechanisms behind the sub-inertial sea level oscillations observed along the Southeast Brazilian coast. These waves are generated south of the study area (Argentina coast) due to atmospheric disturbances and propagate NE, along the Southeast Brazilian shelf.

### **2.2.6 Currents**

Current velocities are mostly driven by tidal forcing, reaching up to 0.5 m/s. Small variations occur between surface and depth-mean currents (Figure 7).

Current patterns in Santos estuary do not present significant differences between winter and summer periods, as they are driven mostly by the tidal forcing (Harari et al., 2008).

According to Harari et al. (2008), tidal waves coming from S. Vicente and Santos meet between sections 6 and 4 (Figure 7). Average current velocities are given in Table 1 for Piaçaguera station (section 5 on Figure 7) where stronger tidal current velocities are observed during spring tides at surface.

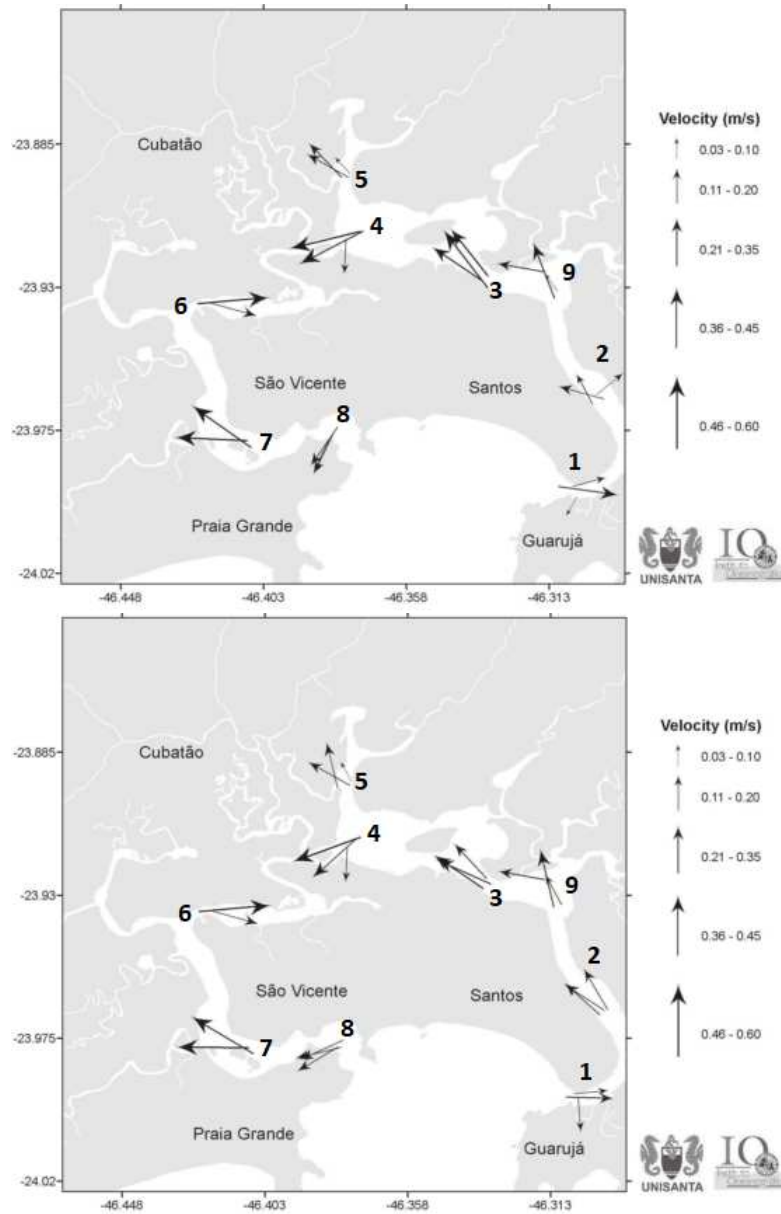


Figure 7: Surface currents (top) and depth mean currents (bottom) based on measurements at several depths on september 2005. Adapted from: Harari et al. (2008).

Table 1: Tidal current velocities in Santos estuary measured in Piaçaguera station ( $23^{\circ}54.0'S;46^{\circ}22.6'W$ ). Adapted from: Harari et al. (2008)

Location	Spring tide		Neap tide	
	Ebb (m/s)	Flood (m/s)	Ebb (m/s)	Flood (m/s)
Surface	-0.45	0.35	-0.27	0.32
In-between (5 m)	-0.35	0.30	-0.22	0.26
Bottom (10 m)	-0.26	0.25	-0.15	0.25

### 2.2.7 Wave regime

Wave measurements for Santos region were analyzed by Tessler et al. (2006) for the periods 1968 to 1969 and 1982 to 1985. Results show that most frequent waves, regarding storm conditions, come from southeast. Wave periods are comprehended on average between 6 and 20 s, with larger occurrence on 9 to 11 s. Wave heights are between 0.5 and 2 m during 90% of the time, being 50% in the interval of 1 to 1.5 m.

A measurement campaign carried in S. Vicente bay by INPH (Instituto Nacional de Pesquisas Hidroviárias) between November 1972 and November 1973, were analyzed by Alfredini (2003) and Farinnaccio et al. (2009). Authors reported waves with average periods of 9 to 11 s and average heights of 1 to 2 m.

### 2.2.8 Water temperature and salinity regime

Water temperature and salinity properties were assessed in September 2005, representing winter conditions (Figure 8), and March 2006, portraying summer conditions (Figure 9), during spring flood-tidal conditions. The results comprise 3 sampling stations namely 1 (entrance of Santos port), 5 (Piaçaguera) and 8 (entrance S. Vicente).

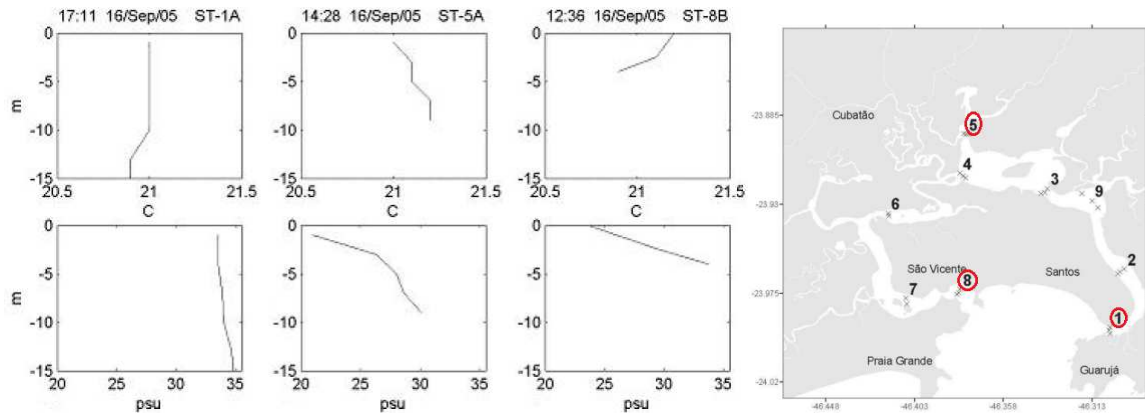


Figure 8: Vertical profiles of water temperature ( $^{\circ}\text{C}$ ) and salinity (psu) in S1, S5 and S8 for September 2005 sampling, representing winter conditions during flood-spring-tide conditions. Adapted from: Harari et al. (2008).

In March, water temperature was significantly higher, ranging between  $26.92^{\circ}\text{C}$  and  $29.12^{\circ}\text{C}$ . Under winter conditions, mean water temperatures were, everywhere in the estuary, close to  $21^{\circ}\text{C}$ , with very small regional variability of  $0.3^{\circ}\text{C}$ . In both seasons, surface and bottom water temperatures display small vertical variations (Harari et al., 2008).

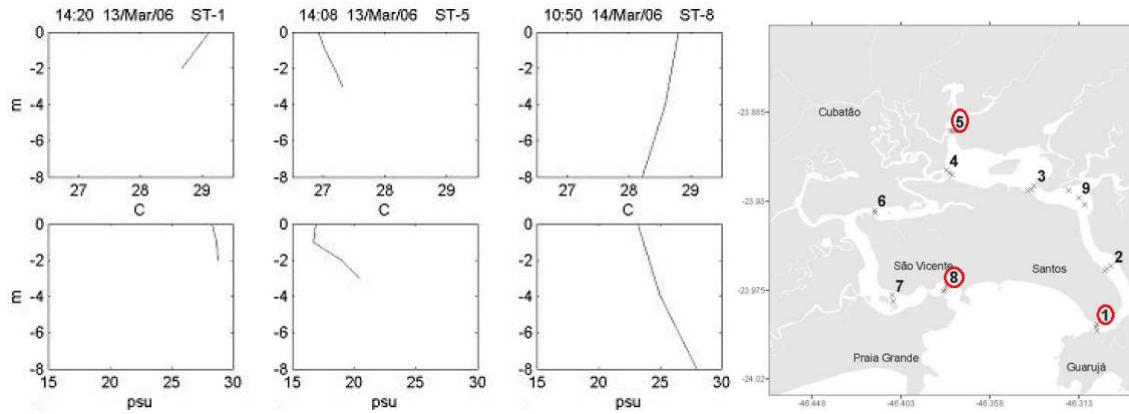


Figure 9: Vertical profiles of physical properties temperature ( $^{\circ}\text{C}$ ) and salinity (psu) in S1, S5 and S8 for march 2006 sampling, representing summer conditions during flood-spring-tide conditions. Adapted from: Harari et al. (2008).

Salinity varies from 15 to 35 psu according to seasonality. Regarding March, salinity values range over a larger interval, from 16.7 to 28.8 psu, whilst in September salinity reached 35 psu at S1. Differences between west (fresh) and east (saltier) estuary entrances should be attributed to the tidal phase. Unlike the water temperature parameter, salinity exhibits significant gradient along the channels and strong vertical stratification in the inner region, up to 4 psu in section 5 (Harari et al., 2008).

According to Harari et al. (2008), the isohalines and isothermals presented in Figure 8 and 9, reveal the salinity as the main density forcing in this system when compared to water temperature.

### 3 The numerical model: MOHID2D

A general overview of the main formulations solved by MOHID is exposed in this section. The modeling governing equations, the bathymetry used, the validation procedure, and detailed information regarding modeling configuration for the Santos estuary application. The hydrodynamic model used throughout this project was MOHID, which was developed in IST. MOHID is a hydrodynamic model designed for coastal and estuarine shallow water applications, like the study of Santos estuary dynamics.

The AQUASAFE platform ([www.aquasafeonline.net](http://www.aquasafeonline.net)), developed by HIDROMOD and distinguished by IWA (International Water Association) was used to extract temporal series used in the present work. AQUASAFE is a software platform supported by modeling tools and advanced data analysis, based on a client-server architecture and developed with a modular philosophy. It can integrate real-time data captured by sensors (local and remote) and run periodically several models (scheduled at user-defined intervals) to produce automatic reports for custom data analysis and comparisons between model predictions and measured data (HIDROMOD, 2016).

#### 3.1 Governing equations

MOHID solves the three-dimensional incompressible primitive equations assuming hydrostatic equilibrium and the Boussinesq and Reynolds approximations. The primitive equations are solved in Cartesian coordinates for incompressible flows. The following equations have been derived taking into account these approximations and more details can be obtained in Santos (1995); Leitão (2003); Vaz (2007). The momentum and mass balance equations are:

$$\frac{\partial u_i}{\partial t} + \frac{\partial(u_i u_j)}{\partial x_j} = -\frac{1}{\rho_0} \frac{\partial p_{atm}}{\partial x_1} - g \frac{\rho(\eta)}{\rho_0} \frac{\partial \eta}{\partial x_1} - \frac{g}{\rho_0} \int_{x_3}^n \frac{\partial \rho'}{\partial x_i} \partial x_3 + \frac{\partial}{\partial x_j} \left( v \frac{\partial u_i}{\partial x_j} \right) - 2\varepsilon_{ijk} \Omega_j u_k \quad (1)$$

$$\frac{\partial u_1}{\partial x_1} + \frac{\partial u_2}{\partial x_2} + \frac{\partial u_3}{\partial x_3} = 0 \quad (2)$$

where  $u_i$  is the velocity vector components in the cartesian  $x_i$  direction,  $v$  the turbulent viscosity,  $\eta$  is the free surface elevation,  $g$  is the gravity acceleration,  $p_{atm}$  the atmospheric pressure,  $\rho$  the density and  $\rho'$  the anomaly,  $\rho(\eta)$  is the free surface density,  $t$  is the time,  $h$  is the depth,  $\Omega$  is the earth velocity of rotation and  $\varepsilon$  is the alternate tensor.

The model transport equation of heat and salt (or any other variable), is given by the



advection-diffusion equation:

$$\frac{\partial C}{\partial t} + u_j \frac{\partial C}{\partial x_j} = \frac{\partial C}{\partial x_j} \left( K \frac{\partial C}{\partial x_i} \right) + FP \quad (3)$$

where  $C$  is the property concentration,  $K$  the diffusion coefficient and  $FP$  is the gain or loss term.

The surface fluxes (important for the heat transport) are composed by the momentum, sensible heat, latent heat, evaporation and infrared radiation (Chapra, 1997). The wind stress is calculated according to:

$$\tau_w^u = \rho_a C_a u_{10} \sqrt{u_{10}^2 + v_{10}^2} \quad (4)$$

where  $\tau_w^u$  is the surface stress induced by the wind,  $\rho_a$  the air density,  $u_{10}$  and  $v_{10}$  are the horizontal components of the wind measured at 10 m height above sea surface and  $C_a$  is the drag coefficient (Riflet et al., 2010). The model horizontal discretization is performed using an Arakawa C grid (Arakawa, 1966), while for the vertical coordinate is used an hybrid and generic scheme, which allows to choose between  $z$ -level, sigma and lagrangian coordinates (Martins et al., 1998; Riflet et al., 2010).

### 3.2 Numerical grids

The numerical grid used for the Santos estuary includes a downscaling approach with four nested levels (L1, L2, L3 and L4), with different horizontal resolutions (Figure 10).

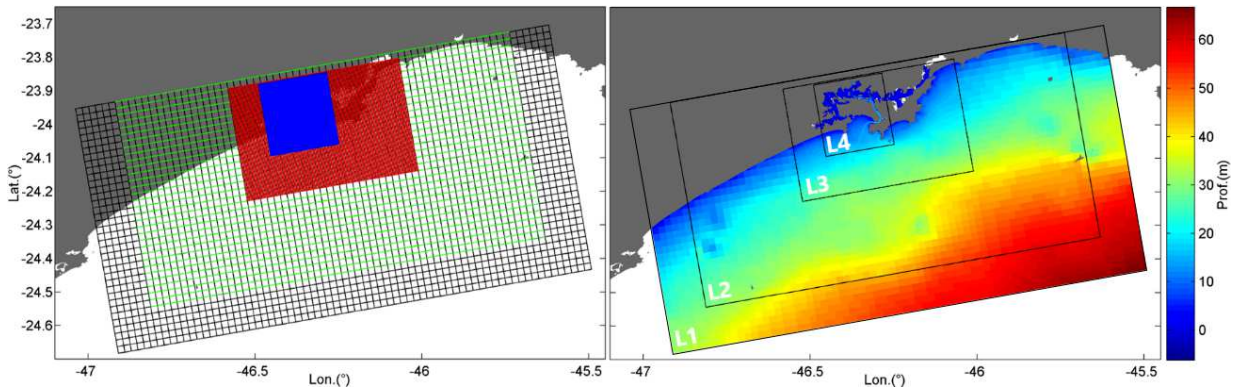


Figure 10: Hydrodynamic numerical grids (left) and bathymetry (right) with 4 levels (L1, L2, L3, L4); the color scale represents the depth in meters. Adapted from: Braga et al. (2016)

The nesting is done only in one way: the large-scale models influences the local models, but not the opposite. The first numerical grid (L1) is a 2D barotropic model, as are the three subsequent grids, using only 1 sigma layer in the vertical dimension and simulating sea level for all domains. L1 ocean boundary was forced by the astronomical tide, calculated from the harmonics of the global tide solution FES2012 (Finite Element Solution). This grid data domain is coarse, since the objective is to simulate large-scale processes (e.g., tide). The second grid is forced at the ocean boundary by the conditions from the L1 grid (high frequency) and low frequency tides coming from the CMEMS (Copernicus Marine Environment Monitoring Service) model (meteorological tide). The conditions generated by the L2 grid are imposed at the boundary of the L3 grid, which provides boundary conditions for the L4 grid. At the surface boundary, all four grids use the results from the meteorological model GFS (50 km) provided by NOAA.

Regarding the grids' characteristics, L1 has a horizontal resolution of  $0.02^\circ$  ( $\sim 2$  km) and  $37 \times 72$  points; L2 has  $31 \times 61$  points and a resolution of  $0.02^\circ$  ( $\sim 2$  km); L3 has a resolution of  $0.004^\circ$  ( $\sim 400$  m) and  $85 \times 130$  points; and the last grid (L4) has a resolution of  $0.0005^\circ$  ( $\sim 50$  m), with  $432 \times 416$  points. A summary of the numerical grids and main characteristics of the implemented model configuration are shown in Table 2.

Table 2: Summary of hydrodynamic model for Santos estuary application.

Domain	L1	L2	L3	L4
Latitude	24.68-23.9°S	24.54-23.9°S	24.22-23.85°S	24.1-23.80°S
Longitude	46.9-45.5°W	46.8-46.0°W	46.5-46.0°W	46.45-46.25°W
$\Delta x$	0.02 °	0.02 °	0.004 °	0.0005 °
Dimensions	$37 \times 72$	$31 \times 61$	$85 \times 130$	$432 \times 416$
Nr of Cells	2664	1891	11050	179712
$\Delta t$	240 s	240 s	120 s	30 s
Horizontal viscosity	20 m <sup>2</sup> /s	4 m <sup>2</sup> /s	4 m <sup>2</sup> /s	0.5 m <sup>2</sup> /s
Tide	FES2012 (6.25 km)	L1+CMEMS	L2	L3
Atmosphere	GFS (50 km)	GFS (50 km)	GFS (50 km)	GFS (50 km)

Present downscaling approach, using 4 nested levels, allows the effects of large-scale atmospheric processes (low resolution) to be imposed in the regional area (high resolution). Therefore, the methodology is capable of simulating processes of different spatial scales on the south-eastern Brazilian shelf, providing accurate boundary conditions to the Santos estuarine system, contributing to model accuracy and efficiency. The most precise domain, L4 ( $\sim 50$  m), allows a better topography and therefore a more approximate description of local processes at Santos estuary.

The bathymetry was obtained by scanning the nautical charts of DHN (Diretoria de Hidrografia e Navegação do Brasil)—1,701; 1,711; 23,100; and 23,200—and by recent surveys conducted by the SP Pilots and NPH-UNISANTA (Núcleo Pesquisas Hidrodinâmicas - Universidade de Santa Cecília) database (Figure 10).

### 3.3 Boundary conditions

Whilst implementing the model, initial and boundary conditions were imposed, specifically oceanic tide and atmospheric conditions. Also, a rugosity of 0.0025 was the value adopted for the following study.

At the oceanic boundary (astronomical tide), the model was forced by FES2012 (Carrière et al., 2012) which is a tidal global solution that provides tidal heights and currents at any location of the world ocean, being widely used in oceanography. This solution has been developed, implemented and validated by the LEGOS, NOVELTIS and CLS, within a CNES funded project. It consists in 32 tidal constituents that are distributed on  $1/16^\circ$  grids (amplitude and phase).

Relatively to meteorological tide, also at the oceanic boundary, it was imposed CMEMS (Lellouche and Regnier, 2015) which provides the download of oceanographic data according to user specifications in NetCDF format. The daily solution was used for the present implementation.

The GFS, available from the NOAA (National Oceanic and Atmospheric Administration), is a meteorological prediction model produced by the NCEP (National Center for Environmental Prediction). For Santos estuary, the daily results of the GFS model are used regarding wind speed and direction, air relative humidity, air temperature, air pressure and precipitation within a horizontal resolution of approximately 50 km.

A summary of the previous mentioned models is presented in Table 3.

### 3.4 Validation

It is an accepted requirement that a numerical model designed to predict estuarine hydrodynamics should be verified, calibrated and validated before used in a practical application (Vaz et al., 2007). For the present work, data ranging from 2016-2017 was extracted from AQUASAFE to validate the model, through comparison between predicted and observed sea level data collected at SP Pilots stations.

Table 3: Global and region numerical modeling network connected to AQUASAFE Santos platform.

Data type	Model	Horizontal resolution	Parameter	Data interval	Source
Meteorological	GFS	50 km	Wind speed and direction, relative humidity air, air temperature, air pressure and precipitation	3 h	NOAA
Tide	CMEMS	8.3 km	Water level (meteorological tide)	24 h	CMEMS
	FES2012	6.25 km	Water level (astronomical tide)	< 1 h	AVISO

## 4 Data and Methodology

This chapter presents the data sets of sea level and wave data, and all the methodologies used to achieve the proposed goals.

### 4.1 Sea level and wave data

Tide measurements collected by 5 tide gauges (with a sampling frequency of 10 min) and wave data (including significant peak wave and period each 20 min) measured at S1, from Santos harbor, are available from 2016-2017. The locations of the 5 stations along Santos estuary and their coordinates can be depicted in Table 4 and Figure 11.

Table 4: Tidal gauges along Santos estuary, coordinates and measured parameters.

Tidal gauges	Designation	Latitude	Longitude	Parameter
Ilhas das Palmas	S1	24°00'81.86''S	46°32'50.94''W	Water level; Wave data
Praticagem	S2	23°99'14.11''S	46°30'17.67''W	Water level
Capitania	S3	23°95'56.79''S	46°30'81W	Water level
Ilha Barnabé	S4	23°92'26.33''S	46°33'35W	Water level
Cosipa	S5	23°87'08.84''S	46°37'81.53''W	Water level

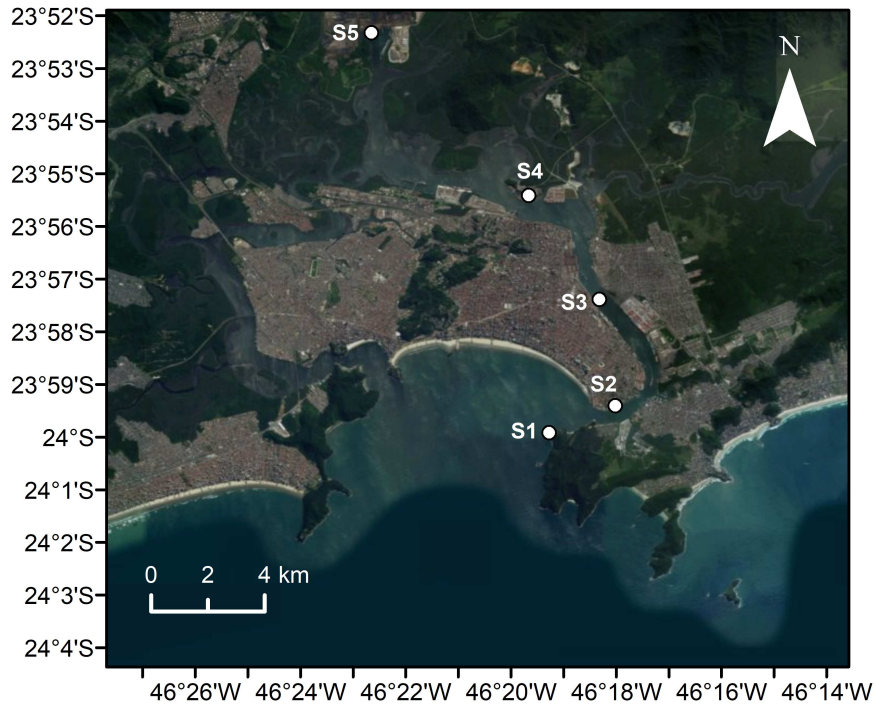


Figure 11: Location of the 5 tide gauges (S1, S2, S3, S4 and S5) along Santos estuary.

The water level data was used to validate model results as well as to perform harmonic analysis. For this purpose, both the sea level and wave database were subjected to several data management procedures such as the outlier correction and data gaps in order to avoid possible residual noise.

The interest of focusing on data gathering in Santos channel relies on the fact of this being the shipping channel. Therefore, no stations in S. Vicente channel and adjoining parts will be discussed, once they are not used for navigation purposes.

## 4.2 Sea level components decomposition

To address sea level problems related to storm surges, the distinct tidal components were addressed individually. The decomposition consisted in separating terms related to sea level height, namely, bias, astronomical tide and residual tide.

### 4.2.1 Bias

Understanding noise and possible bias in tide-gauge sensors is vital for determining the mean sea level, its fluctuations and their engineering implications.

For the Santos estuary, transient differences were found in the equipment vertical reference between tide gauges. For S1 the reduced level is 127.2 cm (2011); S2 is 138.8 cm (2015); S3 is 72 cm (1956); S4 is 113 cm (2017) and S5 is 66.5 cm (2004) considered for a reference datum ([www.portodesantos.com.br](http://www.portodesantos.com.br)) (Figure 12).

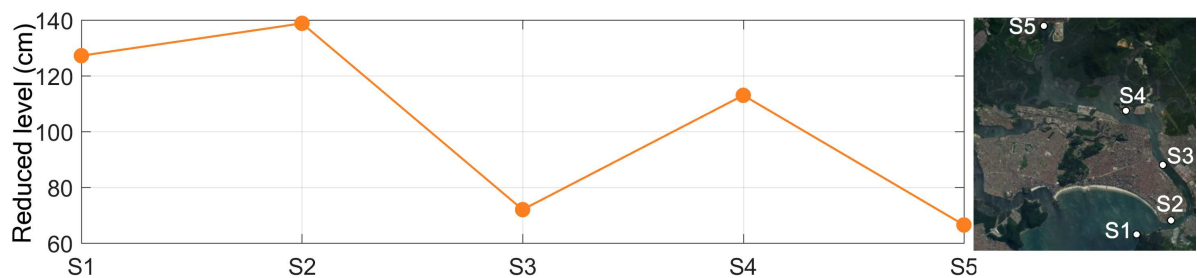


Figure 12: Reduced level (cm) for the 5 tide gauges along Santos estuary. Source: [www.portodesantos.com.br](http://www.portodesantos.com.br)

No apparent physical explanation was found to explain this spatial variability. The uncertainties in vertical reference among the distinct tide gauges can be a limitation for water level prediction. One solution to this issue is to correct both water levels to level zero in post processing phase. Therefore, further analysis will take into account the *UNBIAS RMSE* rather than *RMSE*, as the results may be somehow affected by the

uncertainties related to bias problem. Several literature was found relating problems in continuous sea level records with its associated bias (Doran, 2010; Hamlington et al., 2016). It is assumed that errors related to measurements only arise from systematic referential bias.

#### 4.2.2 Astronomical tide

Errors related to astronomical tide were achieved through direct comparison between astronomical component of predictions and observations datasets. These time series were obtained through reconstruction analysis using T\_Tide package (Pawlowicz et al., 2002) that consists in routines to perform classical harmonic analysis with nodal corrections, plus predictions can be assessed using the analyzed constituents.

Furthermore, harmonic analysis was performed in order to understand which constituents are better predicted as well as their pattern throughout Santos canal. An important feature of this harmonic analysis package is the estimation of the 95% confidence interval associated with each calculated amplitude and phase, leading this software to be widely used by oceanographers.

Having both amplitude ( $A_i$ ) and phase lag ( $G_i$ ) of each constituent, the height of the tide ( $H$ ) can be calculated at any time ( $t$ ) as the sum of contributions of each tidal constituent by the following equation:

$$H(t) = A_0 + \sum_{i=1}^k A_i F_i \cos(\omega_i t + (V_0 + u)_i - G_i) \quad (5)$$

where  $A_0$  represents the mean water level;  $k$  the number of tidal constituents;  $i$  the index of a constituent;  $\omega_i$  the angular velocity and  $(V_0 + u)_i$  the astronomical argument.  $F_i$  and  $u_i$  can be intended as the amplitude and phase corrections.

Table 5 portrays a brief description, frequency and period of the main harmonic constituents that will be taken into account along this work.

Additionally, the Mean Complex Amplitude Error ( $HC_i$ ) is calculated to compare amplitude and phase of each harmonic constituent, as also the relative value of HC ( $RHC_i$ ) parameter (Equations 6 and 7).

$$HC_i = \left\{ \left[ h_{mod_i} \cos(\varphi_{mod_i}) - h \cos(\varphi_{obs_i}) \right]^2 + \left[ h_{mod_i} \sin(\varphi_{mod_i}) - h_{obs_i} \sin(\varphi_{obs_i}) \right]^2 \right\} \quad (6)$$

Table 5: Main harmonic constituents description. Source: NOAA.

Constituent	Description	Frequency ( $^{\circ}/h$ )	Period (h)
M <sub>2</sub>	Principal lunar semi-diurnal	28.98	12.42
S <sub>2</sub>	Principal solar semi-diurnal	30.00	12.00
O <sub>1</sub>	Lunar diurnal	13.94	25.82
K <sub>2</sub>	Lunisolar semi-diurnal	30.08	11.97
K <sub>1</sub>	Lunar diurnal	15.04	23.93
N <sub>2</sub>	Larger lunar elliptic semi-diurnal	28.44	12.66
Q <sub>1</sub>	Larger lunar elliptic diurnal	13.40	26.87
P <sub>1</sub>	Solar diurnal	14.96	24.07
M <sub>3</sub>	Lunar third-diurnal	43.48	8.27
M <sub>4</sub>	Shallow water of principal lunar	57.97	6.21

$$RHC_i = \frac{HC_I}{h_{obs_i}} \times 100 \quad (7)$$

The  $h_{mod_i}$ ,  $h_{obs_i}$ ,  $\varphi_{mod_i}$ ,  $\varphi_{obs_i}$  parameters correspond to amplitudes and phase of predictions and observations, respectively (Chanut et al., 2010). The use of  $HC$  and  $RHC$  is useful for obtaining a comprehensive view of the behavior of each harmonic constant error, individually in terms of its amplitude and phase discrepancies.

Pickard and Pond (1978) introduced the tidal Form Factor ( $F$ ) to evaluate the dominance of diurnal ( $K_1$  and  $O_1$ ) and semi-diurnal ( $M_2$  and  $S_2$ ) components, according to:

$$F = \frac{(K_1 + O_1)}{(M_2 + S_2)} \quad (8)$$

Depending on the result, tide can be classified as semi-diurnal ( $F < 0.25$ ); mixed with mainly semi-diurnal ( $0.25 < F < 1.50$ ); mixed with dominantly diurnal ( $1.5 < F < 3.0$ ); diurnal ( $F > 3.0$ ).  $F$  factor was calculated for both predictions and observations for the 5 tide gauges along Santos estuary.

In order to characterize tidal patterns in Santos estuary, it was calculated the sum of constituents amplitudes (long period, diurnal, semi-diurnal, third-diurnal, quarter-diurnal) to verify if a strong amplification of constituents occurs throughout the channel.

#### 4.2.3 Residual tide

Tide consists in a combination of astronomic and residual tide. Although astronomic tide can be well predicted, residual tide can not and might present an irregular pattern.



When comparing the observed water level at a tide gauge station and the predicted values obtained through harmonic synthesis, there is always a difference that can be related to the contribution of meteorological forcing (storm surges), tide-surge interaction and errors associated with harmonic synthesis and instruments (Pugh (1987); Horsburgh and Wilson (2007); Pugh and Woodworth (2014)).

The approach applied to estimate residuals consists in subtracting the tide synthesized by harmonic analysis and total water level. Thus, the non-tidal residuals were calculated as following (Pugh and Woodworth, 2014):

$$R(t) = X(t) - (Z_0 + T(t)) \quad (9)$$

where  $R(t)$  is the non tidal residual,  $X(t)$  and  $(Z_0 + T(t))$  are the observed and synthesized level, respectively. Other methods include filtering to remove all short periods, to obtain residual elevation without influence from tidal interaction (Horsburgh and Wilson, 2007). It is important to mention that only positive residuals will be considered during the present work.

#### 4.2.4 Statistical analysis of water level

To compare predicted and observed data, several statistical parameters were applied. The *RMSE* calculates the absolute measure of the model deviation from data, being one of the most used error parameter to assess tidal model performance (Dias and Lopes, 2006; Oliveira et al., 2006):

$$RMSE = \left\{ \frac{1}{N} \sum_{i=1}^N [X_{obs} - X_{mod}]^2 \right\}^{\frac{1}{2}} \quad (10)$$

where  $N$  corresponds to the number of records and  $X_{obs}$  and  $X_{mod}$  represent observations and model predictions, respectively.

Considering two dimensional variables,  $X_{obs}$  and  $X_{mod}$ , the Correlation Coefficient ( $R$ ) is expressed as:

$$R = \frac{1}{N} \sum_{i=1}^N \frac{(X_{obs} - \overline{X_{obs}}) \cdot (X_{mod} - \overline{X_{mod}})}{\sigma_{X_{mod}} \sigma_{X_{obs}}} \quad (11)$$

The variables  $\sigma_{X_{mod}}$  and  $\sigma_{X_{obs}}$  represent the variances of  $X_{mod}$  (predictions) and  $X_{obs}$

(observations), respectively:

$$\sigma_{X_{obs}}^2 = \frac{1}{N} \sum_{i=1}^N (X_{obs} - \overline{X_{obs}})^2 \quad (12)$$

$$\sigma_{X_{mod}}^2 = \frac{1}{N} \sum_{i=1}^N (X_{mod} - \overline{X_{mod}})^2 \quad (13)$$

Also, the predictive *SKILL* value was computed, being a descriptive measure that reflects the degree to which the observed variable is accurately estimated by the predicted variable (Willmott, 1981). This index can be mathematically expressed as:

$$SKILL = 1 - \frac{\sum |X_{mod} - X_{obs}|^2}{\sum (|X_{mod} - \bar{X}_{obs}| + |X_{obs} - \bar{X}_{obs}|)^2} \quad (14)$$

where values of 1 correspond to a perfect adjustment between predictions and observations, while values of 0 indicates a complete disagreement. Higher values than 0.95 should be considered excellent (Dias et al., 2009).

For a better portrayal of the statistics, Taylor diagrams were done to provide a concise statistical summary of how well patterns match each other in terms of their correlation coefficient, their *RMSE* difference, and standard deviation. In general, these diagrams characterize the statistical relationship between two fields, a "test" field and a "reference" field (based on observations) (Taylor, 2001).

### 4.3 FES2014 implementation

In the present work, it was tested the novel FES2014 astronomic solution as an oceanic boundary condition for the model. This aimed to test if the newest version would better represent the astronomic tide in Santos estuary. Comparing to FES2012, the newest version takes advantage of longer altimeter time series and better altimeter standards, improved modeling and data assimilation techniques, a more accurate ocean bathymetry and a refined mesh in most of shallow water regions. FES2014 solution, released in 2016, shows strong improvement compared to FES2012, particularly in coastal and shelf regions shallow water constituents. Therefore, it is also intended to verify if any enhancement is observed in the prediction of  $M_3$  and  $M_4$  constituents.

The code used to compute FES2014 was developed in collaboration between LEGOS (Laboratoire d'Etudes en Geophysique et Oceanographie Spatiales), Noveltis, CLS

(Collecte Localisation Satellites) Space Oceanography Division within a CNES funded project, and is available under GNU General Public License.

FES2014 source data, provided by AVISO, were downloaded from [www.aviso.altimetry.fr](http://www.aviso.altimetry.fr). Data is available in NetCDF format and was subject to several modifications and conversions to be imposed according to MOHID specifications. All procedures were done through MATLAB software, allowing a useful and effective handling of the datasets. Thus, the dataset containing amplitude and phase of 34 harmonic constituents, had to be centered in Atlantic region, phases were converted to positive values and amplitudes converted to meters. Lastly, the file was converted to HDF5 format to be used in MOHID.

Having the HDF5 prepared, it was aimed to compare FES2014 solution with the previous version. Therefore, two simulations were performed only considering astronomical tide, ignoring other forcings, the first using FES2012 and other with FES2014. Thus, same boundary and initial conditions were imposed, excepting astronomical tide global solution. Model was set up to run for one year (1st of January of 2016 until 1st of January of 2017) to allow the results to be compared with tidal gauge data analyzed. A hourly time gap was used for these comparisons. As initial conditions, zero free surface gradient and zero velocity at all grid points were used. A warm-up period of one day was considered for both model simulations avoiding numerical instabilities, being the results analyzed after this period.

#### 4.4 CMEMS implementation

The CMEMS (meteorological tide), imposed in model as oceanic boundary condition, was tested with a distinct time resolution. Therefore, hourly model results were assessed with the hypothesis that the 24 h temporal resolution, currently in use, may not be sufficient to forecast some intense residual tide events during short time periods. Dataset is available in <http://marine.copernicus.eu/>, being the time range selected from 01/01/2016 to 01/01/2017, for a geographical area comprehending the S. Paulo coast, being the property downloaded the sea surface height, which corresponds to the meteorological tide.

Two datasets of CMEMS model (hourly and daily) were compared to the tidal gauge data (residual component, after performing the harmonic analysis) to investigate which temporal resolution could better describe the residual tide observed.

Due to the computational time required, it was not possible to repeat MOHID simulations with the oceanic boundary condition CMEMS (hourly resolution) for the an-

alyzed year, with all atmospheric forcings associated. Therefore only the statistical results were evaluated by direct comparison of residual tide observed with daily and hourly datasets extracted from <http://marine.copernicus.eu/>.

## 4.5 Post-processing correction method

It is hypothesized that residual tides forecast errors increase during extreme events (wind, atmospheric pressure and wave regime). It was approached the relationship among physical variables to study their influence on the residual tide. Therefore, it was evaluated the correlation between the residual tides (predictions and observations) with atmospheric (wind intensity, pressure) and oceanographic parameters (significant peak wave). A strong correlation could be found between residual tides (predicted and observed) and wave height.

Thus, each event of  $H_s$  higher than 1.5 m during at least 3h (2016-2017), which was the threshold adopted for the present study, was isolated and studied. For these events, it was found out the maximum level reached by residual tide (predicted and observed). Then, the error was calculated (residual predicted minus residual observed) and a linear regression technique was applied, being the error the dependent parameter whereas  $H_s$  the independent variable.

Through the application of a linear regression technique it was investigated the possibility of correcting residual tide for specific wave height conditions ( $<1.5$  m) in post-processing forecast models. With this purpose, it was linearly added the slope coefficient from regression technique to water level forecast, when  $H_s > 1.5$  m.

Additionally, this method was applied to the hourly temporal resolution, that was implemented since 01/04/2017, for also a period of one year (04/2017-04/2018) to validate again this experiment.

The steps to achieve this goal and the results are described in the following chapter.

## 5 Results and discussion

The present section presents the main results obtained in this work such as: numerical model validation, astronomical tide assessment including the harmonic analysis, tidal propagation characterization, the residual tide assessment, the extreme wave events and, finally the correlation of meteoceanographic properties. Additionally, the applicance of distinct boundary conditions for FES2014 (astronomic tide) global solution and CMEMS (meteorological tide) are tested in the present chapter.

### 5.1 Numerical model validation

The statistical analysis to evaluate model performance (comparison between predictions and observations), for 1 year record can be seen in Table 6, including  $R$ ,  $RMSE$ ,  $UNBIAS RMSE$  and  $SKILL$  parameters. Results for the validation of the local model (Level 4) are depicted for the 5 stations.

Table 6: Statistical parameters ( $R$ ,  $RMSE$ ,  $UNBIAS RMSE$  and  $SKILL$ ) (cm) for water level for the 5 tide gauges in Santos estuary for 2016-2017.

Station	Model	$R$	$RMSE$	$UNBIAS RMSE$	$SKILL$
S1	MOHID Level 4 (50 m)	0.95	12.9	12.5	0.97
S2		0.95	17.9	12.8	0.95
S3		0.94	15.1	14.2	0.97
S4		0.93	17.3	16.9	0.96
S5		0.90	19.9	19.7	0.94

Due to the huge discrepancy in the bias values, namely for S2, all results will be discussed in terms of  $UNBIAS$  values. Figure 13 shows this bias discrepancy in terms of mean sea level for observations and predictions.

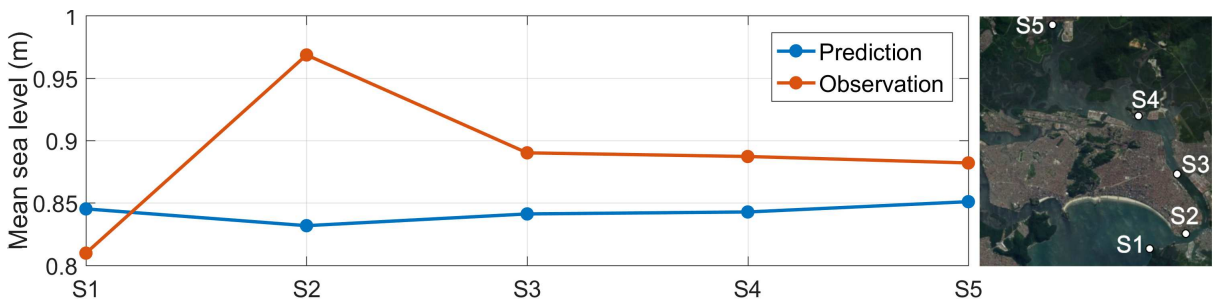


Figure 13: Comparison between predicted and observed mean sea level (m) for the 5 tide gauges along Santos estuary.

Regarding predicted mean sea level, it can be seen that results do not show significant variability among stations. On the contrary, observed mean sea level presents high variability among different stations, particularly for S2. Also, most of stations mean sea level observations are above predictions, except for S1.

In general, it can be seen in Table 6 that results reveal a good agreement between predictions and observations.

According to Dias et al. (2009), a *RMSE* lower than 5% of the local amplitude represents an excellent agreement between model predictions and observations, while an *RMSE* between 5% and 10% indicates a very good agreement.

Errors along the estuary vary from 12.5 cm in S1 (error of 9.6%) until 19.7 cm in S5 (error of 15%), respectively, being minimum *UNBIAS RMSE* value found in the bay entrance. S2 presents an error of 9.8%, S3 around 10.9% and S4 13%. Therefore, S1, S2 stations may be considered with very good agreement. As the distance from the S1 station increases, the deviations between predictions and observations are more evident.

Dias et al. (2009) suggested that water level *SKILL* higher than 0.95 can be considered excellent. Bearing this in mind, an excellent agreement was found for the majority of sites S1, S2, S3 and S4. On the other hand, *SKILL* values higher than 0.90 represent good agreement in which can be included S5.

*R* results range from 0.90 to 0.95, being the best found in S1, S2 and the lower agreement found on S5.

Figure 14 sums up statistical parameters of observations and predictions using Taylor diagrams, namely *UNBIAS RMSE*, Correlation Coefficient and Standard Deviation.

Analyzing the Taylor diagrams, which compare observed data with predictions, it was concluded that sea level is better reproduced for S1 and S2. The *UNBIAS RMSE* for the S1 and S2, is ~12 cm, for S3, S4, S5 the *UNBIAS RMSE* has values between ~15 and ~20 cm. Moreover, lowest *STD* values (~0.38 m) are found for S1 and S2, whereas S5 presents the highest *STD* of ~0.44 m .

Generally, it can be visually depicted that towards the estuary, statistical differences become higher.

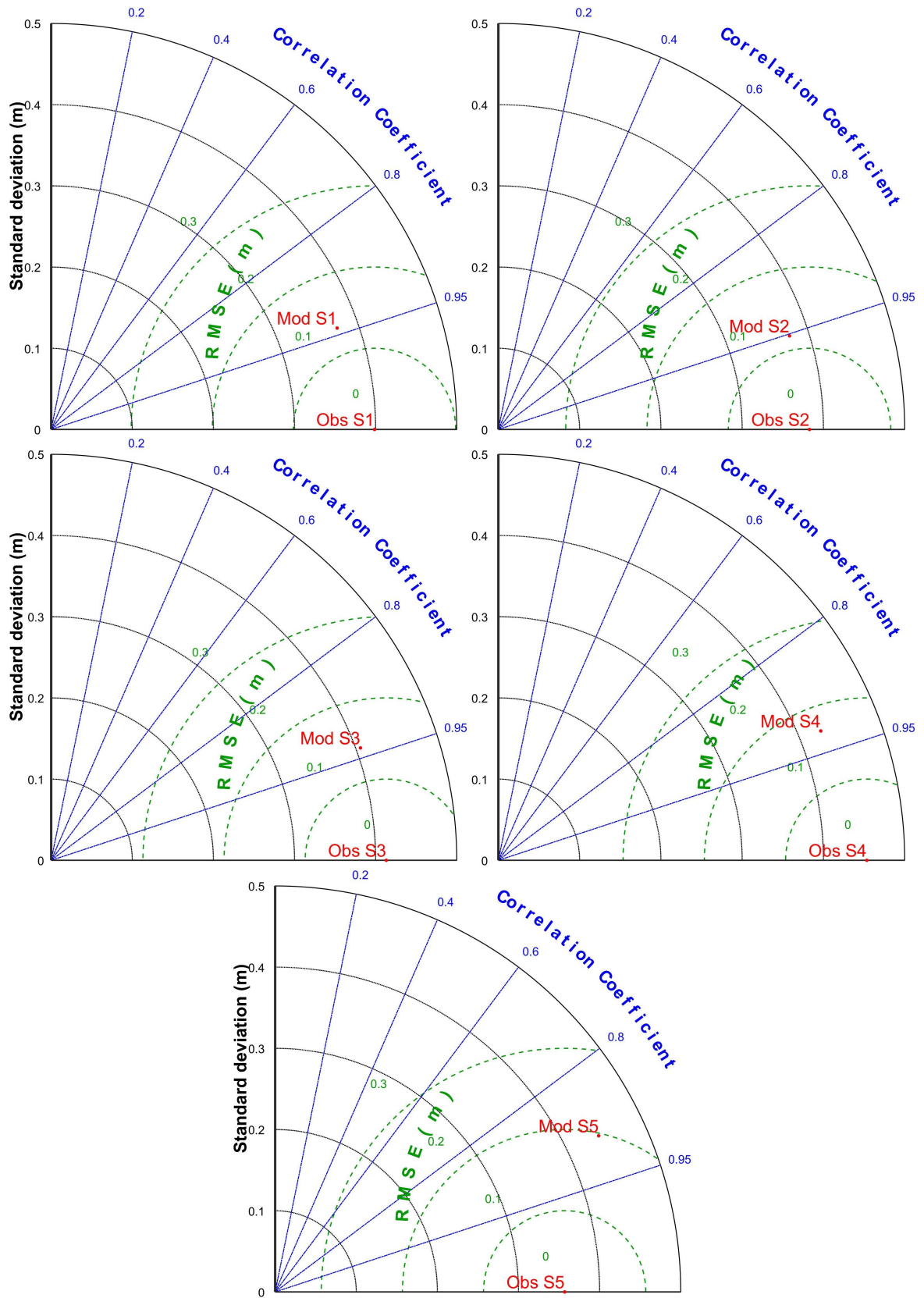


Figure 14: Taylor diagrams for the 5 tide gauges along Santos estuary, including *UN-BIAS RMSE*, standard deviation, correlation coefficient.

## 5.2 Astronomical tide assessment

The statistical analysis to evaluate model performance in terms of astronomical component (predictions and observations), computed for 1 year record is depicted in Table 7, including  $R$ ,  $UNBIAS\ RMSE$  and  $SKILL$  parameters. Results are depicted for 5 study sites along SE.

Table 7: Statistical parameters ( $R$ ,  $UNBIAS\ RMSE$ , and  $SKILL$ ) (cm) for astronomical tide for the 5 tide gauges in Santos estuary for 2016-2017.

Station	Dataset	$R$	$UNBIAS\ RMSE$	$SKILL$
S1		0.98	7.3	0.99
S2		0.98	6.9	0.99
S3	Astronomical tide	0.97	9.9	0.98
S4		0.95	12.9	0.97
S5		0.93	17.4	0.94

It can be noticed that the astronomical tide  $UNBIAS\ RMSE$  values increase towards the inner area. These results may reflect in one hand, the model errors increase in inner areas due to accumulative effect of inaccuracies along the tide wave propagation trajectory. On the other hand, may evidence the low quality bathymetry in the inner estuary, mainly in the mangrove areas. Also, both parameters  $R$  and  $SKILL$  decrease towards the estuary. Although the  $RMSE$  between predictions and observations can be computed to measure model performance, more often the calibration and validation procedures involve some degree of subjectivity. In fact, there is a large disadvantage on the direct comparison of  $RMSE$  errors, since phase errors and amplitude errors are considered together. For example, two datasets with no error in amplitude and a small error in phase can lead to a large  $RMSE$  (Dias and Lopes, 2006). Therefore, it was performed the harmonic analysis.

### 5.2.1 Harmonic analysis

A comparison of amplitude and phases of the main important solar ( $K_1$ ,  $O_1$ ,  $Q_1$ ,  $P_1$ ), lunar ( $M_2$ ,  $S_2$ ,  $N_2$ ,  $K_2$ ) and non-linear ( $M_3$ ,  $M_4$ ) constituents was performed, using the harmonic analysis software T\_Tide (Pawlowicz et al., 2002).

A prior aspect when performing harmonic analysis is to consider a period that should be enough to separate the constituents that present the smaller differences. Therefore, the data sets range from 1st of January 2016 to 1st of January of 2017, encompassing a period of 1 year, which seems to be appropriate for accurate harmonic analysis. Hence, a year time series of 10 min of predicted and observed water level in five tide-gauges



in Santos estuary are compared, aiming to evaluate the model forecasting capacity. It must be pointed out that any gaps in the time series must be filled, so that data can be evenly spaced. So, a special effort was made to eliminate errors and fill gaps to correct discrepancies.

Table 8 represents the principal diurnal, semi-diurnal and non-linear constituents (third-diurnal and quarter diurnal), for a better approach on the main discrepancies among predictions and observations.

Table 8: Harmonic constituents amplitude (cm) and phase ( $^{\circ}$ ) for all stations in Santos estuary for 2016-2017.

		S1		S2		S3		S4		S5	
		Amp	Pha	Amp	Pha	Amp	Pha	Amp	Pha	Amp	Pha
M <sub>2</sub>	Obs	36.6	161.9	35.8	167.7	38.9	170.6	42.8	172.5	33.9	175.6
	Pre	36.2	167.8	37.0	170.4	40.9	176.7	43.4	181.4	46.0	185.3
S <sub>2</sub>	Obs	23.4	169.8	22.7	175.0	24.8	179.1	27.4	181.8	21.6	184.8
	Pre	25.3	177.3	25.8	179.4	28.3	187.1	29.9	192.5	31.6	197.3
O <sub>1</sub>	Obs	11.1	123.2	11.2	124.8	11.4	127.5	11.5	128.0	11.4	133.1
	Pre	11.1	123.2	11.1	124.2	11.4	126.1	11.5	128.0	11.6	129.7
K <sub>2</sub>	Obs	7.3	160.7	7.2	166.0	7.9	168.8	8.7	171.7	6.3	178.0
	Pre	6.9	165.8	7.0	168.2	7.7	175.7	8.1	181.2	8.5	185.9
K <sub>1</sub>	Obs	6.5	183.9	6.5	188.0	6.6	185.3	7.0	182.1	5.5	186.6
	Pre	6.5	184.8	6.6	186.1	6.7	187.5	6.8	189.2	6.8	190.5
N <sub>2</sub>	Obs	4.9	215.4	4.9	221.1	5.4	225.1	5.9	227.4	4.6	232.8
	Pre	4.6	226.9	4.7	229.0	5.1	235.3	5.3	239.9	5.6	244.0
Q <sub>1</sub>	Obs	3.2	93.8	3.2	99.3	3.1	98.5	3.6	97.7	2.6	102.0
	Pre	3.1	99.4	3.1	99.9	3.2	101.9	3.2	103.7	3.3	105.5
P <sub>1</sub>	Obs	2.4	173.9	2.4	177.1	2.6	177.2	2.9	191.6	2.1	184.0
	Pre	2.1	193.7	2.2	195.2	2.2	198.9	2.3	202.2	2.3	205.1
M <sub>3</sub>	Obs	4.8	325.0	4.8	333.5	5.5	340.8	6.5	347.0	5.1	352.0
	Pre	1.7	302.1	1.7	307.1	2.0	320.1	2.2	328.5	2.4	335.4
M <sub>4</sub>	Obs	1.9	149.1	1.6	148.8	2.3	153.7	2.6	143.9	2.4	149.5
	Pre	3.5	232.9	2.8	248.8	2.7	277.7	2.9	302.7	3.4	317.1

For a visual comparison, Figure 15 refers to water level harmonic analysis for both predicted and observed data, with respective bar errors to detect any significant errors in the tidal constituents.

Relatively to the first station (S1), the main constituent, M<sub>2</sub>, is well reproduced, presenting an amplitude error of 0.21 cm and a phase lag of 6.48° (13 minutes). Highest discrepancies are found for S<sub>2</sub> (amplitude error of 2.84 cm and a phase lag of 9.11° (18 minutes)), M<sub>3</sub> (3.14 cm and comprehending a phase lag of 22.94° (32 minutes)) and M<sub>4</sub> (1.51 cm with a phase lag of 83.82° (1h27 minutes)) constituents.

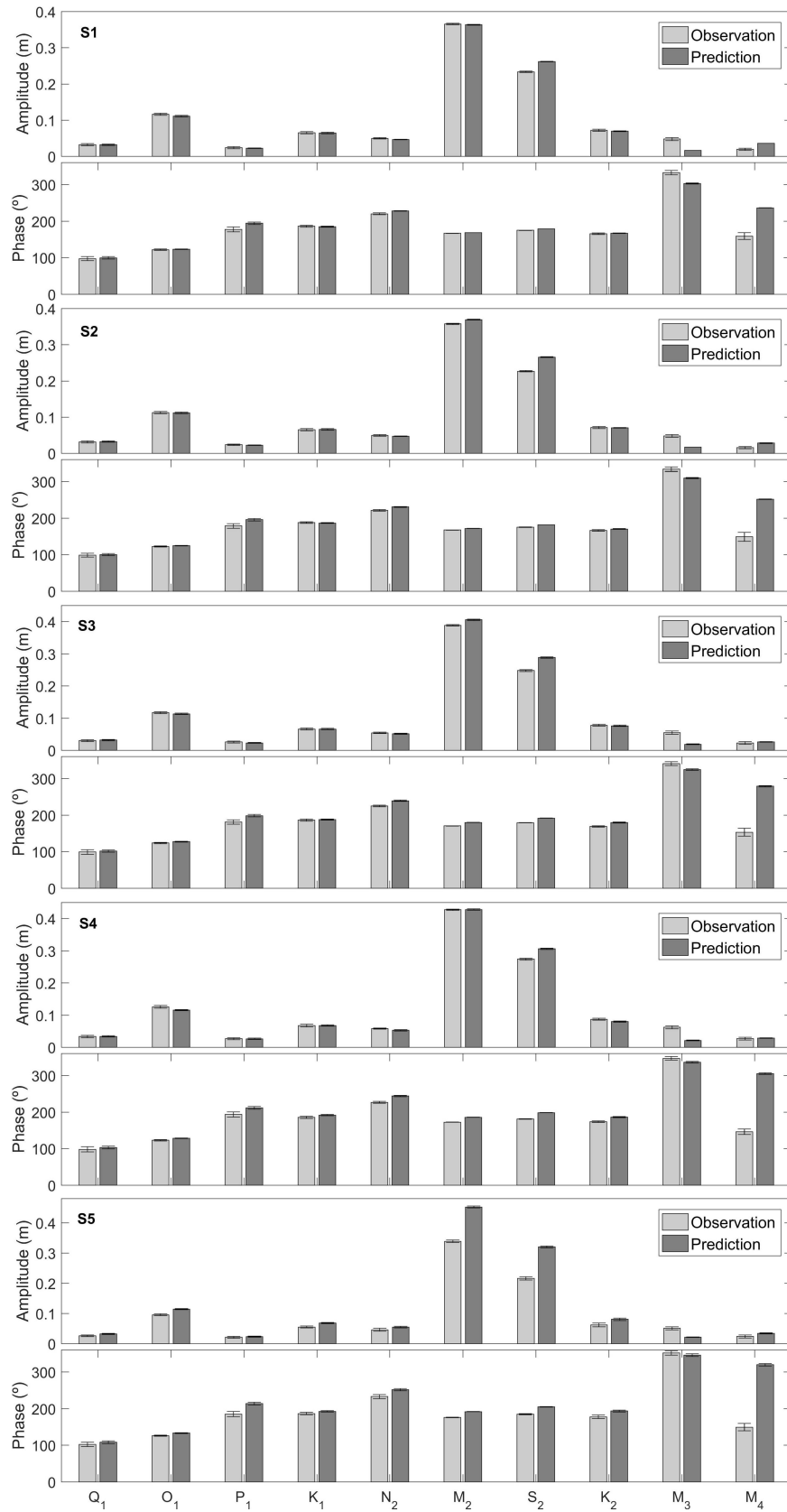


Figure 15: Harmonic constants (amplitude (m) and phase ( $^{\circ}$ )) determined from model predictions and observations, with error bars in the tidal gauges located in Santos estuary.

For  $S_2$  constituent, discrepancies appears to be related to boundary conditions imposed, since predictions are higher than observations at S1 station. For the  $M_3$  constituent, model underestimation of amplitude may reflect uncertainties in the global astronomical solution in terms of Brazilian regional features. It is important to mention that regarding S3, S4 and S5 stations,  $M_3$  is the sixth most important constituent, proving the importance of this constituent amplification in Brazil coast region. Regarding  $M_4$ , model overestimates its amplitude since the bay entrance. Further errors may reflect the bathymetric issues or may arise from  $M_2$  uncertainties.

Regarding diurnal constituents, very good agreement is found in terms of amplitude and phase lag, except  $P_1$  constituent presenting a phase lag of  $19.8^\circ$  (1h19 minutes), being this lag amplified throughout the estuary.

Generally, phase lags and amplitude differences become higher until the end of S5.

### 5.2.2 HC and RHC

Results on the harmonic analysis, using both predictions and observations, clearly show that throughout the Santos estuary the *HC* intensifies as the distance to the bay increases, regarding all constituents in general, as seen in Figure 16. This must be due to the influence of the vast inter-tidal mangrove area of the innermost part of the estuary, where bathymetric information presents some uncertainties.

The major constituents portray the higher discrepancies between predictions and observations, namely  $M_2$  reaches a massive increase at S5 (0.157 cm) followed by  $S_2$ . *HC* values at S1 are less than 0.02 cm for the main constituents, except for  $S_2$  (0.33 cm) and for the shallow water constituents  $M_3$  and  $M_4$  (0.34 and 0.36 cm, respectively).

On the other hand, for *RHC*, major errors were found for non-linear constituents,  $M_3$  and  $M_4$  respectively. In general, for higher amplitude constituents, amplitude and phase difference between observations and predictions are lower. Moreover, differences in phase are observed for the shallow water constituents. From this analysis, it was concluded that the main harmonics are reproduced well since *RHC* are less than 10%. On the other hand, for constituents  $P_1$  ( $RHC > 30\%$ ),  $M_3$  ( $RHC > 50\%$ ), and  $M_4$  ( $RHC > 130\%$ ), were found the largest discrepancies.

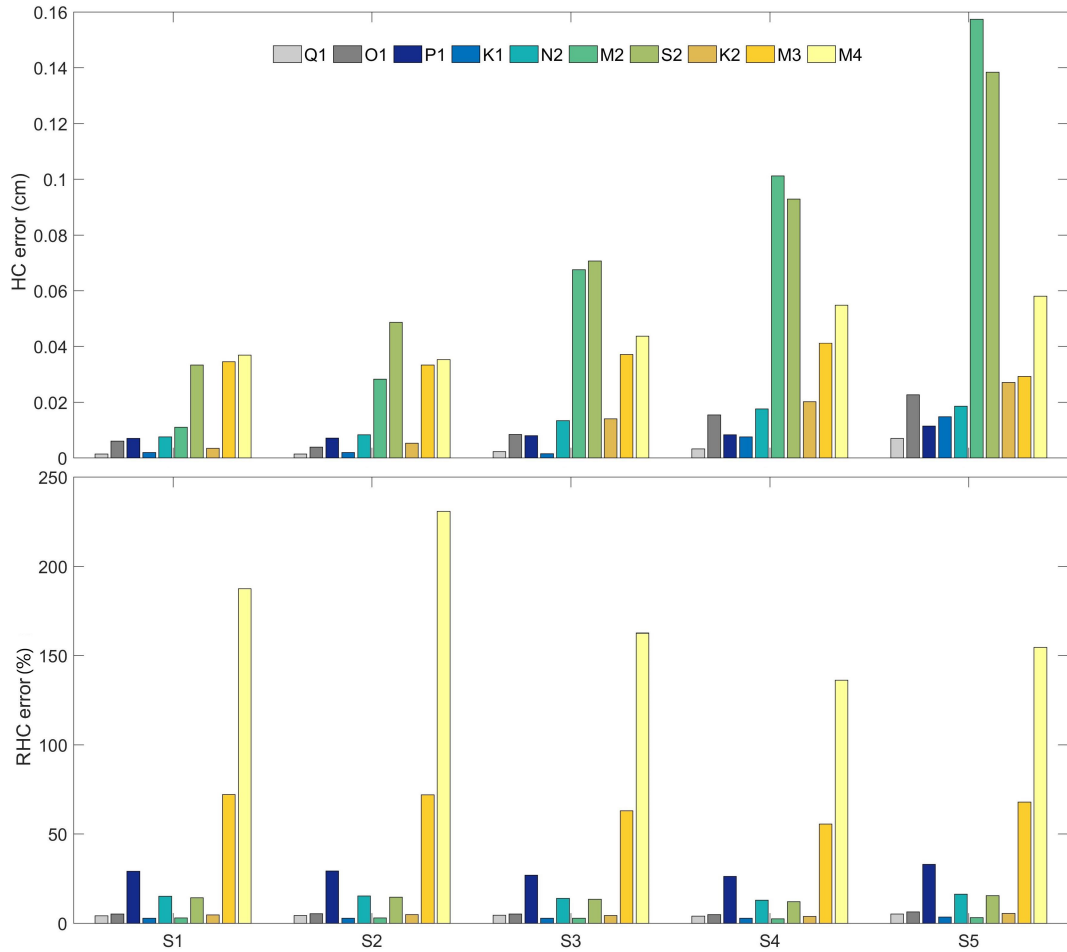


Figure 16: *HC* (top) in cm and *RHC* (bottom) in % error for the 5 tide gauges in Santos estuary for 2016-2017.

### 5.3 Tidal propagation characterization

In order to fully understand the tidal patterns, it is crucial to characterize tidal propagation both from predictions and observations along the Santos estuary.

Form factor was calculated for the 5 stations along Santos estuary, using the harmonic constants determined both from predictions and observations. The results on the tide classification can be depicted in Table 9.

It can be confirmed the mixed mainly semi-diurnal tidal regime of Santos estuary, consisting in two unequal high tides or low tides each tidal cycle, for most of the stations analyzed. Similar results for the study area were reported by Speranzini (2017). On the other hand, station S5 presents a semi-diurnal regime regarding predictions.

Generally, it can be seen an agreement in Form factor determined from predictions and observations. Observations present higher tidal form factor for all stations considered

Table 9: Form factor ( $F$ ) determined from observations and predictions for the 5 tide gauges along Santos estuary.

Station	Form factor	Result
S1	Obs	0.30
	Pre	0.28
S2	Obs	0.30
	Pre	0.28
S3	Obs	Mixed mainly semi-diurnal
	Pre	
S4	Obs	0.28
	Pre	0.25
S5	Obs	Semi-diurnal
	Pre	

( $\sim 0.29$ ) when compared to predictions ( $\sim 0.26$ ). It can be verified that  $F$  decreases from station S1 to S5 stations, both for observations and predictions. These results may relate the dominance of semi-diurnal ( $M_2$  and  $S_2$ ) in comparison to diurnal ( $K_1$  and  $O_1$ ) components, that increases towards the estuary.

The sum of amplitudes and relative importance of the main long period (6), diurnal (21), semi-diurnal (17), third-diurnal (5), quarter-diurnal and other shallow water constituents are presented in Table 10. These values correspond to the five tidal gauges (observations) and comprehend the 68 tidal constituents determined by the harmonic analysis performed.

Table 10: Sum of the amplitudes (m) and relative importance (%) of the main tidal constituents in different frequency bands.

Constituents	S1		S2		S3		S4		S5	
Long period	0.16	11%	0.19	13%	0.20	12%	0.23	13%	0.18	12%
Diurnal	0.29	19%	0.29	19%	0.31	19%	0.36	20%	0.26	18%
Semi-diurnal	0.82	55%	0.81	54%	0.88	53%	0.98	54%	0.78	54%
Third-diurnal	0.12	8%	0.12	8%	0.14	8%	0.16	9%	0.13	9%
Quarter-diurnal	0.07	5%	0.06	4%	0.08	5%	0.11	6%	0.09	6%
Others	0.03	2%	0.03	2%	0.04	2%	0.06	3%	0.06	4%
Total	1.49	100%	1.50	100%	1.66	100%	1.80	100%	1.44	100%

It can be noticed the amplification of total tidal harmonic, from 1.49 m (S1) until 1.80 m (S4) except for the station S5, where a decrease was found. Regarding station S1, diurnal and semi-diurnal constituents are responsible for approximately 74% of the tidal energy in Santos estuary. The significance of  $M_2$  in terms of amplitude is  $\sim 44\%$  for all semi-diurnal constituents considered. On the other hand,  $S_2$  amplitude significance is  $\sim 81\%$  regarding diurnal constituents. The significance of third-diurnal

and quarter-diurnal constituents is noticeable, being  $M_3$  responsible for 40% of total third-diurnal, whilst  $M_4$  contributes with 29% total quarter-diurnal amplitudes. It is clearly observed the importance of the local tidal potential and bottom friction by the amplification of third and quarter-diurnal constituents throughout Santos estuary. A similar pattern was reported by Franz et al. (2016) for the Paranaguá estuarine system. Amplitude and phase charts for the most important semi-diurnal ( $M_2$ ,  $S_2$ ) and shallow water ( $M_3$  and  $M_4$ ) constituents, from the 2016-2017 model predictions are presented in Figures 17 and 18.

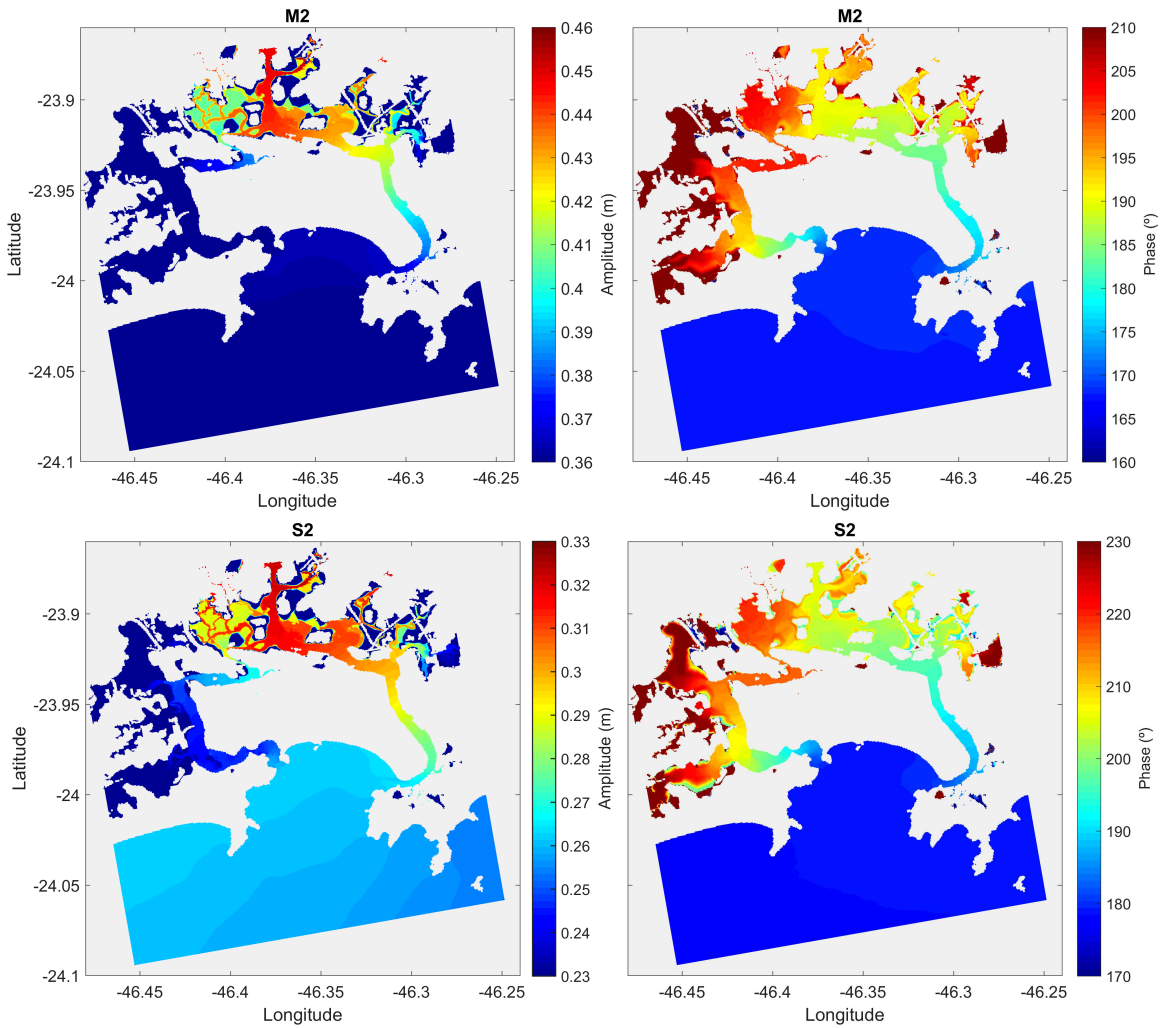


Figure 17: Distribution of  $M_2$  (top) and  $S_2$  (bottom) amplitude and phase for Santos estuary for 2016-2017.

The analysis of these charts provides better characterization of the study area in terms of the spatial distribution of the most important semi-diurnal and non-linear harmonic constituents. It is also important to visualize how model propagates the solution. Scales

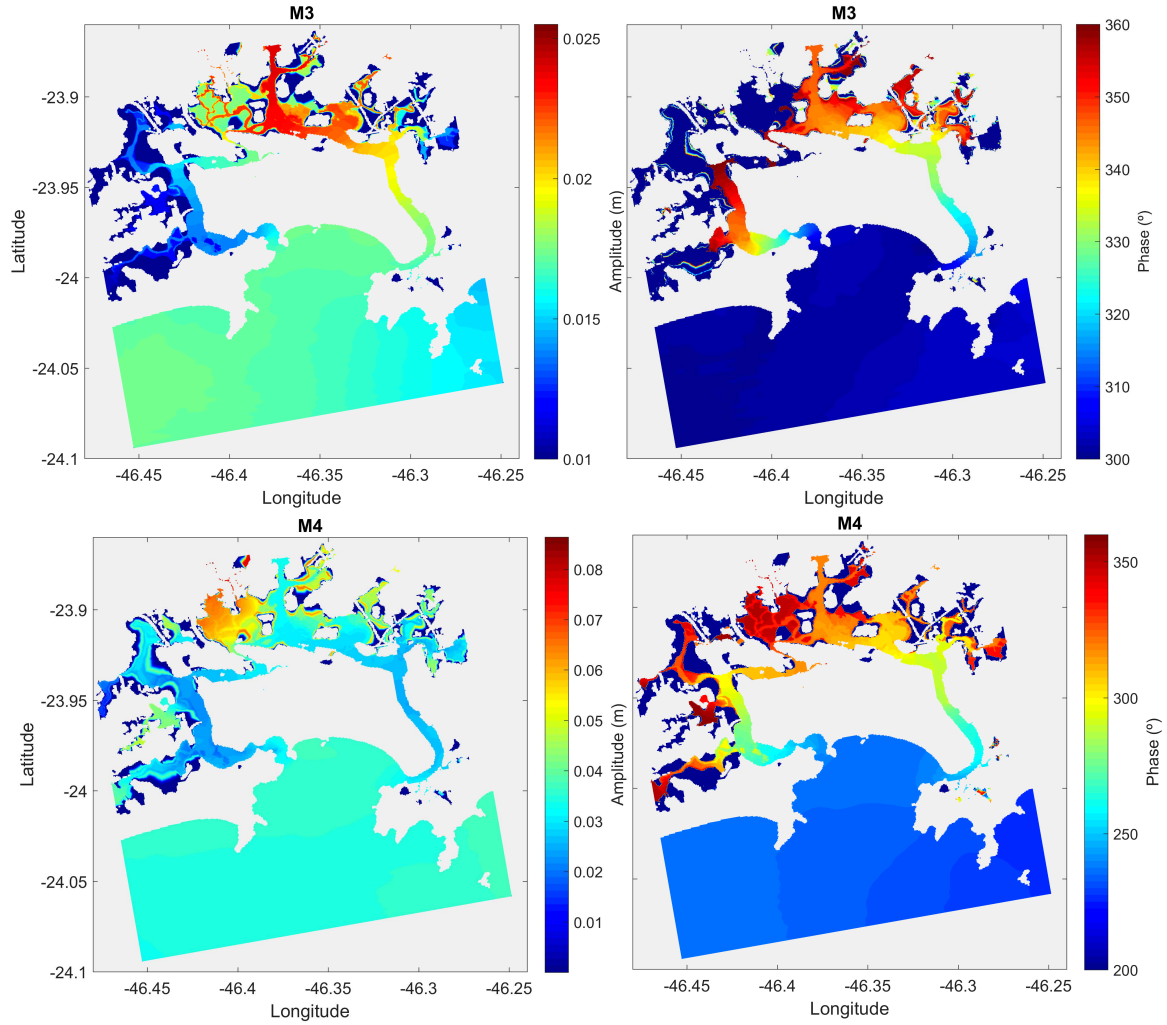


Figure 18: Distribution of  $M_3$  (top) and  $M_4$  (bottom) amplitude and phase for Santos estuary for 2016-2017.

are plotted focusing on the channel where tidal gauges are located, whilst ignoring S. Vicente channel.

A remarkable amplification of the three constituents ( $M_2$ ,  $S_2$  and  $M_3$ ) throughout Santos estuary was found, being maximum values located in Piaçaguera channel.

$M_2$  amplitudes range from 0.36 to 0.46 m, and phase from  $\sim 170$  to  $190^\circ$ .  $S_2$  amplitudes are between 0.25 m at the bay entrance, reaching  $\sim 0.32$  m near the far end of the Santos channel, whilst phases oscillate between  $\sim 177$  to  $197^\circ$ .

Regarding the most important non-linear constituents,  $M_3$  amplitudes range between 0.17 and 0.25 m at the channel ending, whilst phase changes between  $\sim 233$  to  $315^\circ$ . For  $M_4$ , the amplification is less evident in the Santos channel, 3.4 to 3.5 m, whereas phase increases from  $\sim 230$  to  $315^\circ$ . Unlike the other components ( $M_2$ ,  $S_2$  and  $M_3$ ), maximum amplitudes are found west of Piaçaguera channel ( $\sim 6.5$  cm).

Results show that tidal phase and amplitude increases with the distance to S1 as tide propagates along the estuary, specially at the far end of the channels, which are narrow and shallow areas.

## 5.4 Boundary conditions assessment: FES2014

Present subsection will describe the results of the two simulations performed to assess the model performance comparing FES2012 and FES2014 solutions with observations, in terms of astronomical tide.

Table 11 summarizes the harmonic constituents (amplitudes and phases) comparison between observations and both model simulations using FES2012 and FES2014 solutions. The differences correspond to observations minus predictions from the application of FES2012 and FES2014, respectively.

Table 11: Harmonic constituents amplitude (cm) and phase ( $^{\circ}$ ) differences for the 5 tide gauges in Santos estuary for 2016-2017 for FES2012 and FES2014 solutions.

		S1		S2		S3		S4		S5	
		Amp	Pha	Amp	Pha	Amp	Pha	Amp	Pha	Amp	Pha
M <sub>2</sub>	FES12	0.4	-5.8	-1.2	-2.7	-2.0	-6.1	-0.57	-8.87	-12.1	-9.7
	FES14	0.3	-4.8	-1.1	-3.2	-1.4	-7.0	0.56	-11.62	-10.9	-13.5
S <sub>2</sub>	FES12	-1.9	-7.5	-3.1	-4.21	-3.5	-7.9	-2.49	-10.7	-10.0	-12.5
	FES14	-0.6	-6.6	-1.3	-4.8	-2.1	-9.4	-1.37	-13.7	-9.5	-15.2
O <sub>1</sub>	FES12	0	0.08	0.02	0.6	-0.01	1.4	0.01	-0.02	-0.2	3.4
	FES14	-0.1	1.2	-0.1	1.8	-0.12	2.2	-0.11	0.61	-0.3	4.2
K <sub>2</sub>	FES12	0.4	-5.1	0.09	-2.2	0.2	-6.9	0.59	-9.45	-2.3	-7.9
	FES14	0.4	-8.6	0.2	-6.0	0.3	-10.1	0.73	-13.23	-2.1	-13.1
K <sub>1</sub>	FES12	0.04	-0.9	-0.1	1.9	-0.07	-2.2	0.23	-7.07	-1.4	-3.9
	FES14	-0.28	1.3	-0.03	4.1	-0.4	-0.3	-0.09	-5.31	-1.7	-2.6
N <sub>2</sub>	FES12	0.4	-11.6	0.2	-7.9	0.3	-10.2	0.55	-12.55	-1	-11.2
	FES14	0.2	-13.0	-0.4	-4.7	0.5	-8.5	1.08	-10.76	0.2	-11.2
Q <sub>1</sub>	FES12	0.08	-5.6	-0.01	-0.7	-0.1	-3.5	0.38	-6.04	-0.7	-3.5
	FES14	0.2	-4.5	0.2	0.3	-0.01	-3.3	0.47	-6.14	-0.6	-4.4
P <sub>1</sub>	FES12	0.2	-19.9	0.2	-18.1	0.4	-21.7	0.64	-10.6	-0.2	-21.1
	FES14	0.5	3.5	0.4	5.1	0.6	1.5	0.9	12.73	0.06	2.0
M <sub>3</sub>	FES12	3.1	22.9	3.0	26.5	3.5	20.7	4.26	18.5	2.6	16.7
	FES14	3.6	19.0	3.0	23.9	4.3	20.3	5.26	17.7	3.9	14.0
M <sub>4</sub>	FES12	-1.5	-83.8	-1.2	-100	-0.4	-124	-0.3	-158.8	-1.0	-167.6
	FES14	-0.4	13.5	-0.9	14.7	-1.6	-1.9	-2.1	-21.3	-3.6	-25.4

The implementation of FES2014 showed better agreement between harmonic constants determined from predictions and observations for the main constituents, at S1 and S2



stations (accuracy is improved 0.1 and 1.27 cm for  $M_2$  and  $S_2$ , respectively). Generally, for the remaining diurnal ( $O_1$ ,  $K_1$ ,  $P_1$ ,  $Q_1$ ) and semi-diurnal ( $N_2$ ,  $K_2$ ) constituents were found slightly worse results.  $M_3$  constituent is worst reproduced by FES2014 in terms of amplitude ( $\sim 0.5$  cm), but improved in terms of phase ( $\sim 4^\circ$ ). Regarding the most important quarter-diurnal constituent ( $M_4$ ), results are more concordant with tidal gauge data in terms of amplitude ( $\sim 1.1$  cm) and phase. In general, the use of FES2014 results in better agreement between model predictions and with *in-situ* data for tide gauges located closer to the estuary mouth.

Additionally,  $HC$  and  $RHC$  were calculated, providing a better visual comparison (Figure 19). Scale ranges were kept the same such as in Figure 16 for a proper comparison.  $M_4$  constituent presents the best improvement according to its amplitude and phase values ( $RHC > 30\%$ ). Remaining constituents present, in general, better results according to these statistical results.

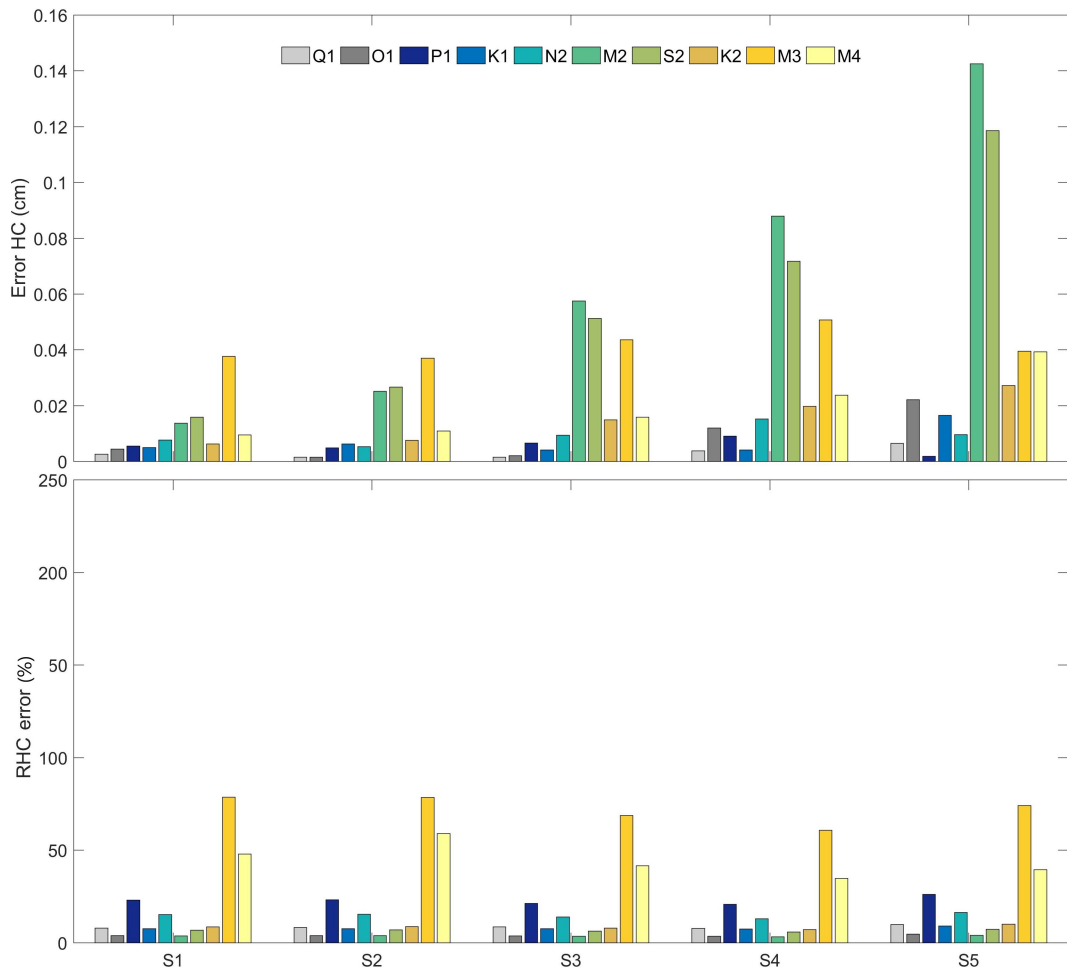


Figure 19:  $HC$  (top) in cm and  $RHC$  (bottom) in % error for the 5 tide gauges in Santos estuary for 2016-2017 with the new implementation of FES2014.

## 5.5 Residual tide assessment

The statistical analysis to evaluate model performance in terms of the determined residual component (predictions and observations), for 2016-2017, is depicted in Table 12, including  $R$ ,  $UNBIAS\ RMSE$  and  $SKILL$  parameters. The estimation of residuals (predicted and observed) were obtained by harmonic subtraction method, as previously mentioned. Results are depicted for 5 study sites along SE.

Table 12: Statistical parameters ( $R$ ,  $UNBIAS\ RMSE$ , and  $SKILL$ ) (cm) for residual tide determined for the 5 tide gauges in Santos estuary for 2016-2017.

Station	Dataset	$R$	$UNBIAS\ RMSE$	$SKILL$
S1		0.87	11.0	0.90
S2		0.89	9.68	0.92
S3	Residual tide	0.89	12.1	0.92
S4		0.91	10.3	0.92
S5		0.85	9.48	0.91

The statistical analysis was performed in order to understand the residual errors variability towards the estuary. It can be observed that  $UNBIAS\ RMSE$  remains practically constant along stations, between 9.48 and 12.1 cm in S5 and S3, respectively.  $R$  values oscillate between 0.85 (S5) and 0.91 (S4) whereas  $SKILL$  values are comprehended between 0.90 (S1) to 0.92 (S2, S3, S4) respectively.

The fact that the residual  $UNBIAS\ RMSE$  along the estuary does not show significant differences can reveal that major errors may be related to the astronomic tide. On the other hand, these results prove that if predictions are improved on the Santos bay, this will be reflected on the stations towards the estuary.

In the coastal zone of S. Paulo, outside the estuary, the dynamics of sub-inertial atmospheric forced events is dominant, with time scales that vary between 4 and 8 days (Chambel and Mateus, 2008). Therefore, residual tidal energy is concentrated on daily perturbations, not being influenced by bottom friction unlike astronomical tide (hourly period).

### 5.5.1 Boundary conditions assessment: CMEMS

Taking into account that residual errors are constant in the estuary, an effort will be made to improve predictions at Santos bay. This subsection will discuss the statistical analysis results of direct comparison of the use of a hourly or daily resolution (CMEMS) with observations (residual tide), aiming to determine if predictions are improved.

For a better perception of the distinct temporal resolution, Figure 20 portrays the hourly and daily residual tide provided by CMEMS (predicted) with residual tide (observed) for S1 station for three distinct time periods (18/04/2016 to 08/05/2016; 10/08/2016 to 28/08/2016; 15/09/2016 to 05/10/2016).

Analyzing Figure 20, it is suggested an evident improvement of the forecast capacity under extreme events, regarding the use of hourly forecasts. Periods of stronger events of residual tide were chosen, to better perceive the use of distinct temporal resolutions. It can be seen that hourly CMEMS resolution better describes the observed residual tide, particularly the positive peaks (e.g. 27/04 and 26/09).

The statistical analysis of residual tide observation and CMEMS daily and hourly model was assessed and results can be depicted in Table 13.

Table 13: Residual tide comparison between observations (S1) daily and hourly CMEMS ( $R$ ,  $RMSE$ ,  $UNBIAS\ RMSE$ ,  $SKILL$ ) results for S1 in Santos estuary.

Data (S1)	$R$	$RMSE$	$UNBIAS\ RMSE$	$SKILL$
Observation - CMEMS (Daily)	0.89	14.0	10.5	0.86
Observation - CMEMS (Hourly)	0.91	13.1	9.28	0.89

The hourly solution improves the forecast capacity under extreme events comparing to the daily solution. The implementation of a higher temporal resolution regarding CMEMS, clearly decreased the error ( $UNBIAS\ RMSE$ ), and improved  $R$  and  $SKILL$  statistical parameters.

This analysis strongly advises the use of CMEMS hourly solution as an oceanic boundary condition in MOHID setup. Errors are only presented for S1 station, but as the residual errors remain constant along Santos channel, it is inferred that for all stations regarding Santos estuary, errors would decrease.

### 5.5.2 Investigating residual tide errors

In this study, the forecast of residual tides is hypothesized to be underestimated during extreme events that usually coincide with storm conditions characterized by intense variability of metocean conditions (e.g. atmospheric pressure, significant wave height, wind velocity).

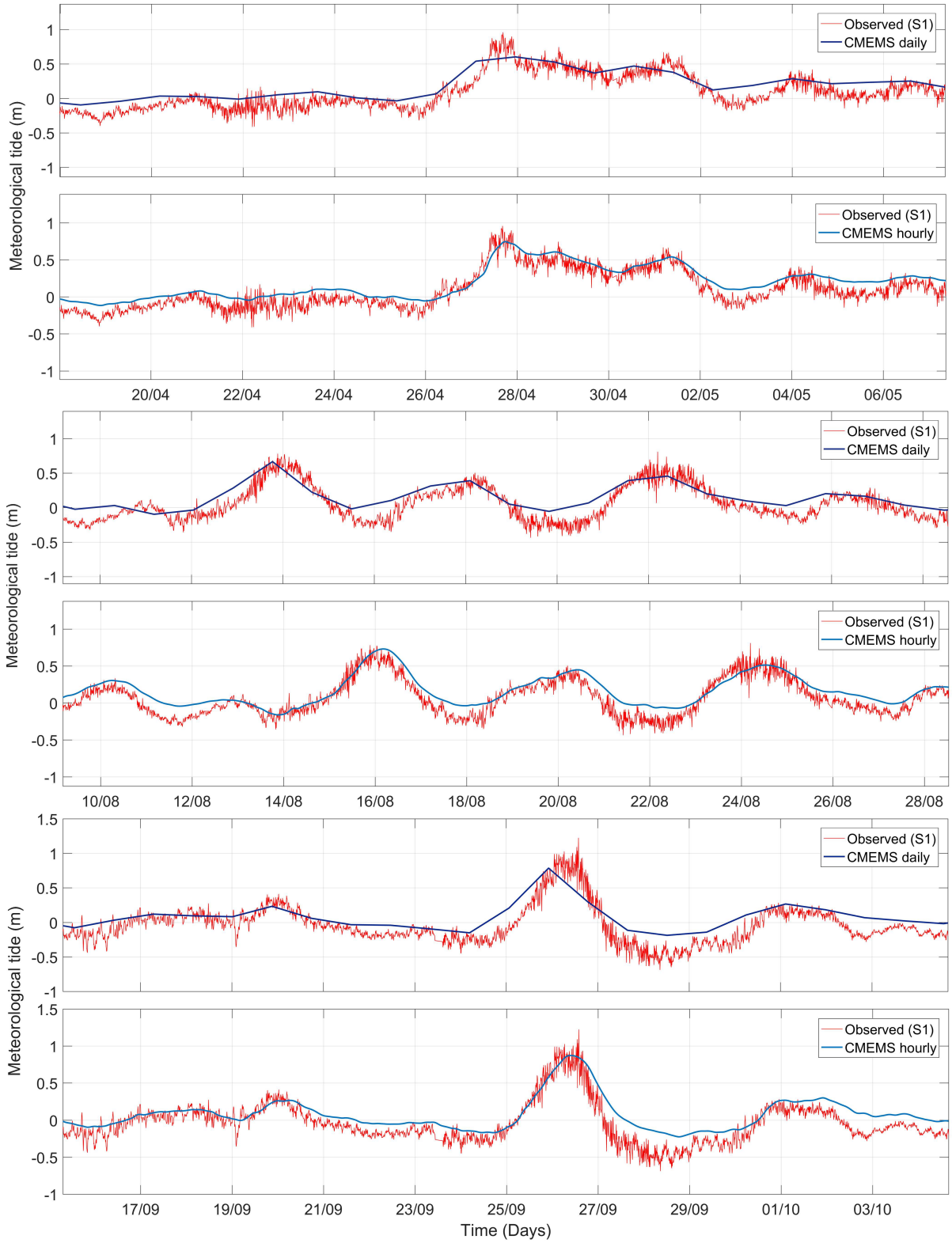


Figure 20: Residual tide observed for S1 station (observations) and CMEMS (predicted): daily and hourly resolution for 3 distinct time periods (18/04/2016 to 08/05/2016; 10/08/2016 to 28/08/2016; 15/09/2016 to 05/10/2016).

Thus, the effect of important changes on meteoceanographic variables in the sea level forecasts was evaluated through the correlation analysis among residual tide and the variables atmospheric pressure, wind intensity and significant wave height. For both atmospheric pressure and wind (direction and intensity) variables, correlations were not conclusive. However, a strong correlation was found for the significant wave height (Figure 21).

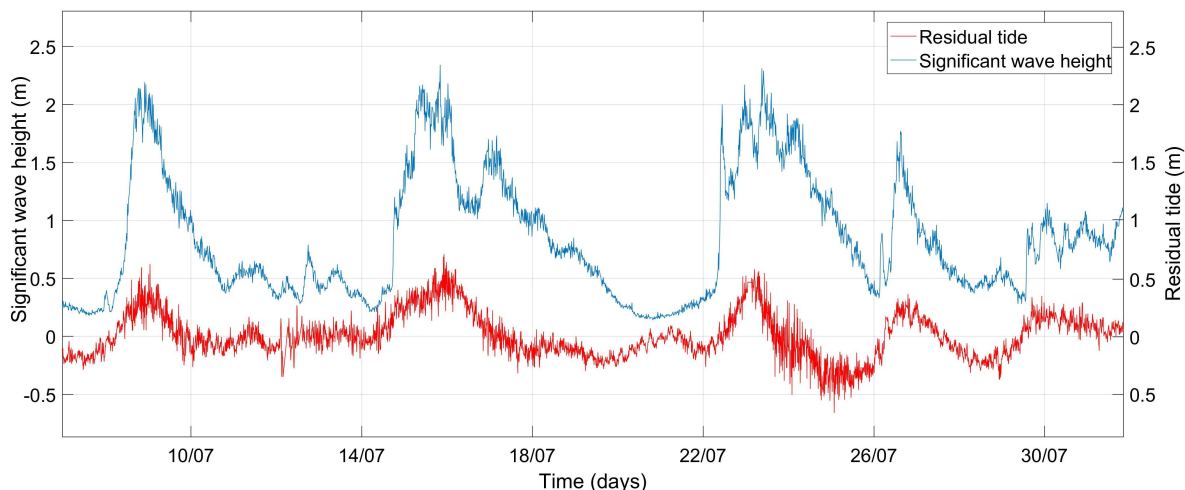


Figure 21: Comparison between observed significant wave height and residual tide determined for S1 station.

### Wave influence hypothesis

Observations of residual tide patterns comparing to significant wave height evolution led to a working hypothesis that waves could somehow influence the sea level values (e.g. wave setup, wave-currents interaction) under storm conditions.

Thus, the statistical analysis correlation between significant wave height (observed) and residual tide (predicted and observed) was assessed for the 5 tide gauges of Santos estuary.

Table 14 presents a pronounced correlation between residual tide (predicted and observed) and significant wave height (observed), being the maximum found in S2 (0.65). Also, correlations are higher for residual tide observations comparing with residual tide predictions.

From this analysis, was concluded that the correlation observed is not related mainly with a direct action of waves because the correlation is also found in the predictions that do not considered any wave effect in model implementation. However, the correlation tends to be higher in the observations ( $\sim 0.64$ ) than in the predictions ( $\sim 0.61$ ). This

might indicate that a second order effect directly associated with waves action may occur in the observations that it is not being considered in simulations.

Table 14: Correlation coefficient between residual tide (predictions and observations) and  $H_s$  (observation).

Station	Dataset		$R$
S1		Obs	0.64
		Pre	0.61
S2		Obs	0.65
		Pre	0.61
S3	Residual tide VS $H_s$	Obs	0.64
		Pre	0.61
S4		Obs	0.65
		Pre	0.62
S5		Obs	0.62
		Pre	0.61

Therefore, it was further investigated the occurrence of extreme events (considering  $H_s$  higher than 1.5 m), and their effect on the residuals.

It was calculated the error of water level forecast once  $H_s$  is higher than 1.5 m. Table 15 shows residual tide *UNBIAS RMSE* for total time series (2016-2017) which is 12.10 cm and the *UNBIAS RMSE* for the indexes of  $H_s > 1.5$ , being 23.77 cm. This proves that forecast errors increase  $\sim 11.67$  cm during storms.

Table 15: Statistical analysis (*UNBIAS RMSE*) of residual tide (cm) for total time series and for  $H_s$  higher than 1.5 m.

Dataset	Model	<i>UNBIAS RMSE</i>	<i>UNBIAS RMSE</i> ( $H_s > 1.5$ )	Difference
Residual tide	CMEMS <sub>daily</sub>	12.10	23.77	11.67

### Post-processing correction - proposed method

Extreme events were carefully studied, depicting the maximum level reached by the storm. Therefore, the wave regime for the period of 2016-2017 was analyzed, and 25 events were found as extreme events characterized by heights greater than 1.5 m and during at least 3 hours (Figure 22).

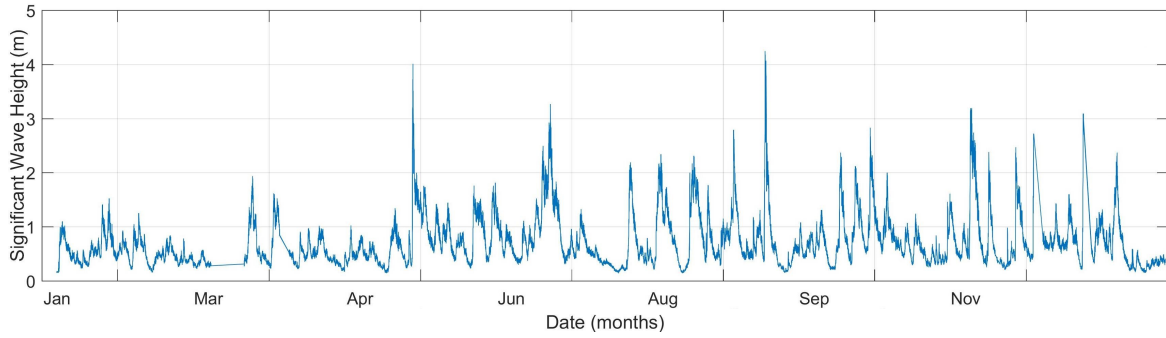


Figure 22: Significant wave height data observed at S1 station in Santos Estuary for 2016-2017.

For the 25 events, it was computed the maximum height reached observed. Additionally, for the same periods of strong wave height, the corresponding maximum values of residual, both observed and predicted, were estimated. After, values were ordered by increasing significant wave height and the error (residual predicted minus residual observed) was calculated (Table 16).

Generally, for increasing values of  $H_s$ , it is seen that residuals observations are higher, however, the same is not observed for predictions. For the most extreme  $H_s$  events (maximum heights of 4.01 and 4.25 m) was also found highest errors (0.356 and 0.496 cm).

Besides, a regression technique was applied to the dataset of Table 16, being the significant wave height the independent parameter versus error as the dependent parameter. Figure 23 presents the regression technique applied between  $H_s$  and residual error.

Table 16: Maximum residual tide (predicted and observed) for extreme events of maximum value of  $H_s$  (m) and respective residual error (m).

$H_s$ (m)	Pre (m)	Obs (m)	Error (m)
1.60	0.157	0.276	0.118
1.62	0.160	0.243	0.084
1.73	0.060	0.123	0.064
1.75	0.202	0.468	0.266
1.76	0.320	0.542	0.222
1.77	0.006	0.241	0.235
1.81	0.129	0.482	0.353
1.93	0.053	0.128	0.074
2.0	-0.063	0.105	0.168
2.0	0.040	0.182	0.142
2.12	0.232	0.427	0.196
2.19	0.102	0.40	0.298
2.31	0.130	0.461	0.331
2.34	0.227	0.483	0.255
2.37	0.485	0.655	0.170
2.37	0.242	0.49	0.249
2.38	0.046	0.238	0.192
2.47	0.182	0.383	0.20
2.72	0.307	0.584	0.277
2.79	0.191	0.373	0.182
2.83	0.345	0.542	0.197
3.19	0.517	0.897	0.381
3.27	0.315	0.648	0.332
4.01	0.496	0.852	0.356
4.25	0.279	0.775	0.496

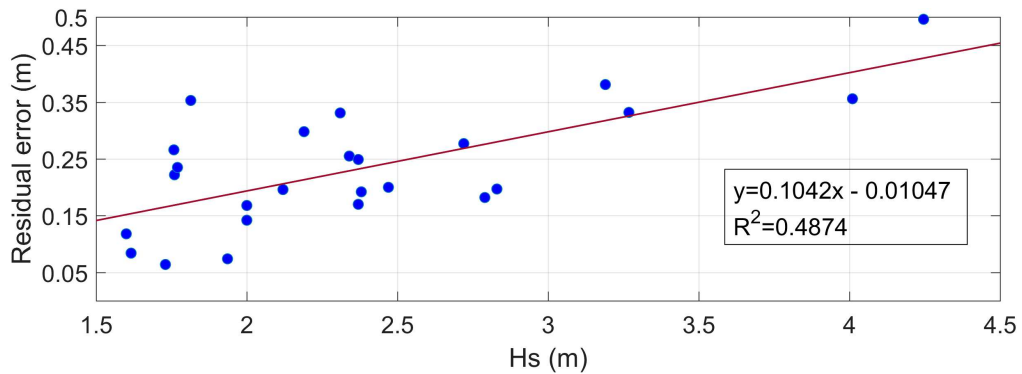


Figure 23: Linear regression between  $H_s$  (m) and residual error (m).

Therefore, it was tested the addition of the slope coefficient (0.1042) to the water level



forecasts once measured  $Hs$  is higher than 1.5 m through the following equation:

$$Water_{level} = Water_{level} + 0.1042 \times Hs_{measured} \quad (15)$$

The statistical analysis of applying the correction factor (equation 15) can be seen in Table 17. It can be compared the *UNBIAS RMSE* related to water level forecast, during high wave activity, with and without the correction factor.

Table 17: Statistical analysis (*UNBIAS RMSE*) of residual tide for  $Hs$  higher than 1.5 m with and without correction factor.

Dataset	Model	<i>UNBIAS RMSE</i>	<i>UNBIAS RMSE</i> <sub>correction</sub>	Difference
Residual tide	CMEMS <sub>daily</sub>	23.77	12.89	10.88

The application of the correction factor improved the results in 10.88 cm, decreasing the *UNBIAS RMSE* from 23.77 to 12.89 cm.

Figure 24 represents the correction applied for the period 2016-2017 for model, model correction, observation and  $Hs$  indexes higher than 1.5 m. Analyzing Figure 24 it can be visually depicted that model correction (orange line) values are closer to observations (yellow line).

The regression technique applied comprehends forecasting residual tide using direct inclusion of significant wave height data during storms. This assumes that the non-periodic residual tide, under certain weather condition in the future, is somehow a repetition of the non-periodical tidal variations under similar meteorological conditions in history.

In the scope of this section, some authors defend the importance of considering the  $Hs$  forcing in the hydrodynamic models. For example, Araújo et al. (2011) investigated the effect of wave set-up on the storm surge water levels at Viana do Castelo for a storm that occurred 14th -16th October (1987), with offshore significant wave height up to 7 m and 13 s peak period. According to the results, wave set-up raised the local water level in 16 cm, contributing for the residual peak 38% when compared to the pressure and the wind. Analyzing Figure 25, it can be seen the importance of this wave effect when comparing the observations with predictions including the effect of pressure and wind, or including pressure, wind and wave set-up.

This proves the wave-setup as a very important phenomenon in hydrodynamics near the coast, causing a significant local elevation of the water level. These results suggest that there is a certain nonlinear transfer of energy between tidal and meteorological forcings, meaning that these dynamics are not completely independent. Authors suggest the

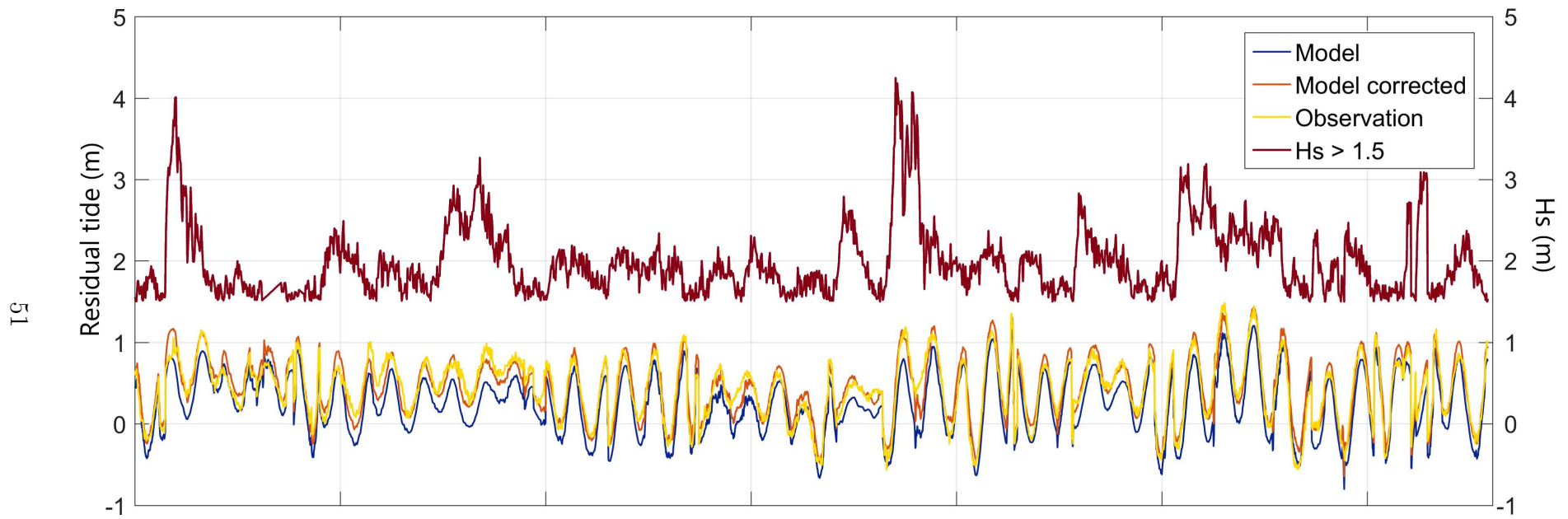


Figure 24: Indexes of  $H_s$  (brown) higher than 1.5 m, model predictions (blue), model with correction factor (orange) and observations (yellow) of residual tide for the year of 2016-2017.

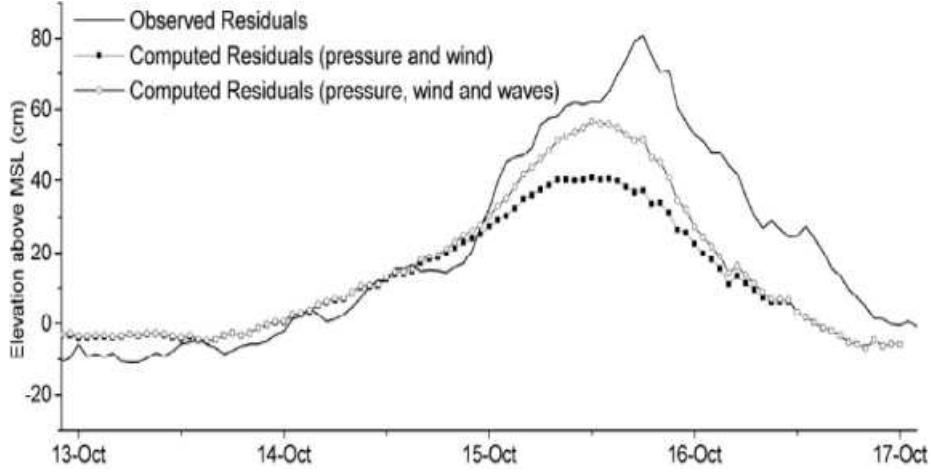


Figure 25: Comparison between observed residual and computed residual (considering pressure and wind and considering pressure, wind and wave setup) for a storm event that occurred in 14-16 Oct. (1987). Adapted from: Araújo et al. (2011).

coupling of tides, atmospheric pressure, wind and wind waves is mandatory under storm surge cases.

### Testing for hourly CMEMS solution

The application of a correction factor to water level forecasts for the analysis of 2016-2017, using CMEMS daily solution, has proven its efficiency. Therefore, it will be tested the same application regarding water level forecasts for 01/04/2017 to 01/04/2018, since modeling results are setup with CMEMS hourly solution.

The method applied allowed to understand the coefficients range, that should be added to water level forecast, under extreme events. Therefore, using MATLAB, it was tested a range of coefficients between 0.1042 and 0.01 to identify which value would result in minimum *UNBIAS RMSE* for the present dataset. The slope coefficient that would result in minimum *UNBIAS RMSE* was 0.022 as seen by following equation:

$$Water_{level} = Water_{level} + 0.022 \times Hs_{measured} \quad (16)$$

Table 18 shows *UNBIAS RMSE* errors related to sea level forecasts during high wave activity periods ( $Hs > 1.5$ ) with and without correction factor (equation 16). The application of a correction factor, improved the results in  $\sim 1$  cm, decreasing the *UNBIAS RMSE*. The *UNBIAS RMSE* values ( $Hs > 1.5$ ) decreases, as expected by the use of CMEMS hourly resolution, previously discussed. However, the post processing correction is still valid, although this application can be considered negligible ( $\sim 1$  cm).

Table 18: Statistical analysis (*UNBIAS RMSE*) of residual tide for  $H_s$  higher than 1.5 m with and without correction factor.

Data set	Model	<i>UNBIAS RMSE</i>	<i>UNBIAS RMSE</i> <sub>correction</sub>	Difference
Residual tide	CMEMS <sub>hourly</sub>	13.15	12.38	0.77

Figure 26 shows correction applied for model, model correction, observation tide and  $H_s$  indexes higher than 1.5 m for the year of 2017-2018.

As seen before, the use of CMEMS hourly model decreased the errors, specifically considering positive residuals events. The imposed correction is reduced since model implementation better represents the residual tides observed as also may have corrected other terms than just the wave influence on water level, such as wind influence. Therefore, storm waves may be a proxy of meteo effects in the Santos estuarine area.

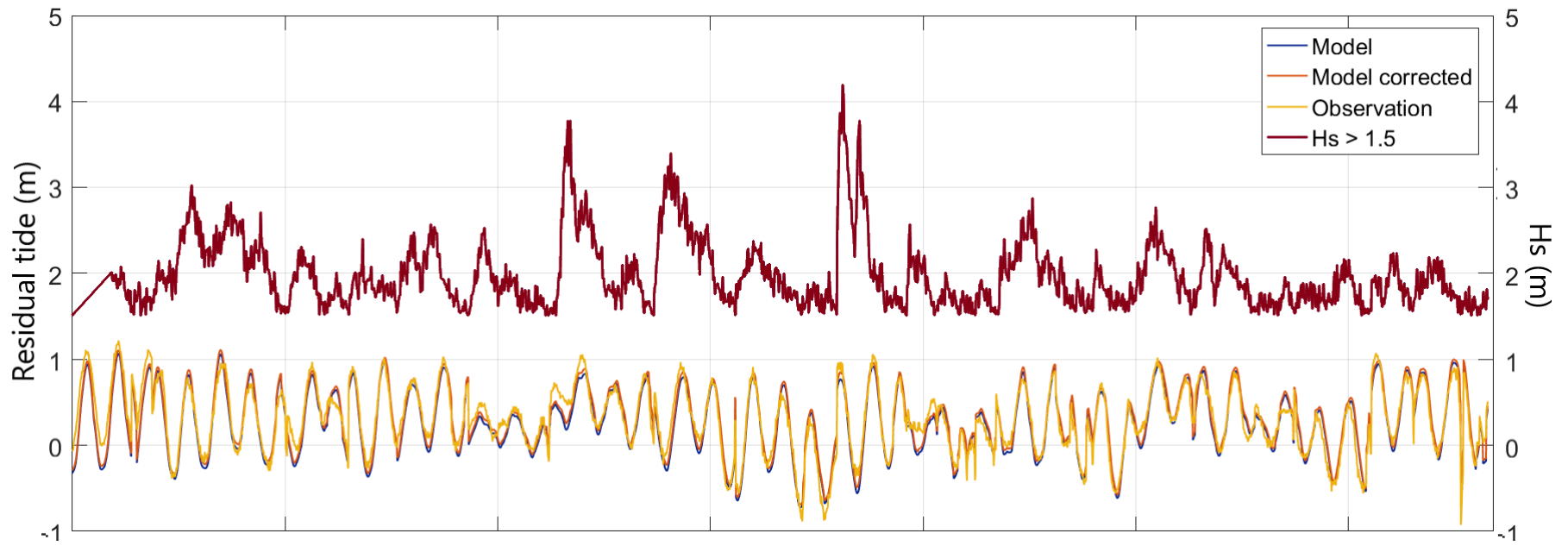


Figure 26: Indexes of  $H_s$  (brown) higher than 1.5 m, model prediction (blue), model correction (orange) and observations (yellow) of residual tide for the year of 2017-2018.

## 6 Conclusion

This dissertation was conducted with the aim of providing new insights about Santos estuary hydrodynamics, as also to optimize the forecast capacity of models currently in use in AQUASAFE platform, particularly for water level under extreme events conditions. To achieve this, a set of objectives were defined, being the main conclusions presented in this section.

The tidal propagation characterization predictions showed that strong amplification occurs for most constituents regarding all stations. The same pattern is verified for observations, however an amplitude decrease was found for the station S5. Model validation was performed for 2016-2017, being the forecast accuracy comprehended between 12.5 to 19.7 cm. Briefly, harmonic analysis portrayed the model errors increase towards the inner estuary and the misrepresentation of  $M_3$ , which is a very particular feature of the Brazilian shelf. On the other hand, residual errors do not show significant differences along the Santos estuary. The individual study of distinct components that comprise water level allowed to improve the forecast capacity for each component (astronomic and residual).

A very important component of the operational services is to guarantee a trustable astronomic tide to impose as oceanic boundary of the forecasting models. The differences between the harmonic constituents found in model predictions and observations arose because of the inaccurate boundary tidal forcing. The constant development of a more accurate global tidal atlas will contribute to further improve model results regarding tidal propagation.

Concerning the astronomical features, the application of FES2014 resulted in several improvements in the astronomical boundary forcing optimizing the harmonic predictions. Advantages of using FES2014, a global hydrodynamic tide solution, instead of local measurements include more robust results independent of local data. Furthermore, FES2014 assimilated altimetry data can be considered a reliable worldwide reference (at least in open ocean). Although, errors remain in shallow waters, being this a limitation of these databases. It can be concluded that global model should consider regional configurations such as  $M_3$  constituent.

For the residual component two hypothesis were tested: study the impact of improving the meteorological oceanic boundary (CMEMS) or assess the possibility to correct data results in post processing stage. The implementation of a hourly temporal resolution instead of daily allowed to better forecast extreme events in Santos estuary, decreasing the errors. Additionally, the methodology developed for detecting the increment in the

water level allowed a post-processing correction, proving its efficiency in operational oceanography.

This work also emphasizes the importance of accurate field measurements that better represent the natural processes and complex ocean system interactions and are necessary to fully validate model set-up.

Regarding the thesis objectives, several improvements were achieved that clearly improved the forecasting capacity for Santos Estuary in reproducing water level evolution, comparing to the previous version..

Although, at Santos estuary, some limitations must be addressed such as bathymetric uncertainties, unsatisfactory spatial and temporal meteorological data resolution, and insufficient data regarding river and dam discharges. The complexity of this drainage basin and the lack of river discharges measurements turn difficult the calculation of freshwater input to Santos estuary.

Problems related to astronomical tide inside Santos channel mainly rely on the poor bathymetric data available for the present area. Some large discrepancies observed at inner tide gauges show the potential lack of accuracy in the bathymetry data. Therefore, there is need for higher resolution bathymetric data to perform the grid refinement in order to capture detailed estuary features. The application of the novel FES solution enlightens the need of new bathymetric data in Santos bay by the fact that at the entrance of the estuary predictions are more concordant with observations. However, for inner stations in the estuary, results are not so concordant. These restrictions strongly affect the forecast capacity of the models as well as compromise the management efforts of Santos coastal area.

A special focus was given to simulation Level 4 (the most precise domain), although it would be also interesting to analyze upper levels.

Though Santos presents a complex tidal regime, in a future study, a more careful analysis of the residual data regarding interaction with atmospheric properties would be recommended. Additionally, to predict residual behavior in advance, previous meteorological data and future forecasts are necessary. In this sense, the application of a neural network could recognize in a more efficient way the atmospheric influence on residual tides would be advisable.

A simulation combining the new implemented boundary conditions with FES2014 and CMEMS (hourly solution) as regional conditions for astronomical and meteorological tide would be advisable, in order to quantify effectively the improvements suggested in this work.

Present work only considered positive residual events, which are extremely important in coastal flooding. However, negative residuals are also important in Santos estuary and may compromise navigation purposes. Therefore, the analysis of negative residuals would also be advisable as future research.

Based upon the evidence that waves induce modifications in water level forecast, it is suggested to study the inclusion of the gradient of the radiation stresses, caused by waves, in the present hydrodynamic implementation. Therefore, the wave influence on residual tides would be explicitly simulated by the model.

Plus, sometimes in Santos estuary, an intense south wind that quickly rotates to west occurs, causing perturbations on the tidal wave and delaying its propagation. This results from highly variable wind characteristics (direction and intensity) during short periods of time due to local complex topography in this region. Also, large scale models can not represent accurately this micro-scale process, particularly related to wind in this area, remaining this issue as a research theme for the future. It is suggested the use of a high resolution meteorological model to test if it would improve local wind forecast and its implication in water level perturbations.

Additionally, model set-up modifications can be used for the investigation of important issues, such as the transport of sediments and water quality. Future research suggestions would include the need to develop extensive databases of several physical and biogeochemical parameters. Taking advantage of AQUASAFE, datasets regarding oceanographic properties can be used to perform further studies. Also, the methodology described in this study can be replicated for other important estuarine systems located on the Brazilian shelf, such as Guanabara bay and Paranaguá bay.

To conclude, for the present AQUASAFE implementation, it is suggested the use of FES2014 global solution in the oceanic astronomic boundary condition for MOHID setup, since it shows better results at the tide gauges closer to inlet. Additionally, it is recommended the use of the CMEMS hourly resolution as an oceanic meteorological boundary condition for MOHID application since it better describes the residual tide positive peaks. On the other hand, it may be used the CMEMS daily resolution as an oceanic meteorological boundary condition, associated with the correction factor, for extreme events of  $H_s$  in the water level forecast, which requires less computational effort (due to lower time resolution).



## References

- Alfredini, P. (2003). O clima de agitação ondulatória na Baía de São Vicente (SP). Technical Report, 11.
- Arakawa, A. (1966). Computational design for long-term numerical integration of the equations of fluid motion: Two-dimensional incompressible flow. Part I. *Journal of Computational Physics*, 1(1):119–143.
- Araújo, M., Mazzolari, A., and Trigo-Teixeira, A. (2011). Wave set-up in the modeling of storm surge at Viana do Castelo (Portugal). *Journal of Coastal Research*, SI 64 (Proceedings of the 11th International Coastal Symposium), 971–975.
- Berzin, G., Leitão, J. C., and Neves, R. (1997). Modelação matemática no Estuário de Santos e sua importância no controle da poluição por águas residuárias. In 19<sup>o</sup> Congresso Brasileiro de Engenharia Sanitária e Ambiental, ABES, Foz do Iguaçu.
- Berzin, G., Leitão, J. C., and Neves, R. (1999). Modelação Hidrodinâmica, uma ferramenta para a gestão de áreas costeiras: o caso do Estuário e Baía de Santos. In XIII Simpósio Brasileiro de Recursos Hídricos, Belo Horizonte (MG), Brasil.
- Braga, R. R., Leitão, J. C., Leitão, P. C., Puia, H. L., and Sampaio, A. P. F. (2016). Integration of high-resolution metocean forecast and observing systems at Port of Santos. In PIANC - COPEDEC 2016, 13.
- Campos, R. M., Camargo, R., and Harari, E. J. (2010). Caracterização de eventos extremos do nível do mar em Santos e sua correspondência com as reanálises do modelo do NCEP no sudoeste do Atlântico Sul. *Revista Brasileira de Meteorologia*, 25(2):175–184.
- Carrère, L., Lyard, F., Cancet, M., Guillot, A., and Roblou, L. (2012). FES2012: A new global tidal model taking advantage of nearly 20 years of altimetry. In: Proceedings of meeting “20 Years of Altimetry”, 6.
- Chambel, J. and Mateus, M. (2008). D2 . 3 – Calibration of the hydrodynamic model for the Santos Estuary. Technical report, 35.
- Chanut, J., Galloudec, O. L., and Léger, F. (2010). Towards North East Atlantic Regional modelling at 1/12° and 1/36° at Mercator Ocean. In Mercator Ocean Quarterly Newsletter, 34:4-12.

- Chapra, S. C. (1997). *Surface water-quality modeling*. New York (N.Y.), McGraw-Hill, 844.
- de Sousa, E., Roberto Tommasi, L., and João David, C. (1998). Microphytobenthic primary production, biomass, nutrients and pollutants of Santos Estuary (24°S, 46°20'W). São Paulo, Brazil. *Brazilian Archives of Biology and Technology*, 41:27–36.
- Dias, J. and Lopes, J. (2006). Calibration and validation of hydrodynamic, salt and heat transport models for Ria de Aveiro lagoon (Portugal). *Journal of Coastal Research*, SI3(39):1680–1684.
- Dias, J. M., Sousa, M. C., Bertin, X., Fortunato, A. B., and Oliveira, A. (2009). Numerical modeling of the impact of the Ancão Inlet relocation (Ria Formosa, Portugal). *Environmental Modelling & Software*, 24(6):711-725.
- Doran, K. J. (2010). Addressing the problem of land motion at tide gauges. PhD thesis, University of South Florida, 116.
- FAPESP (2015). <http://agencia.fapesp.br/inundacoes-costeiras-em-santos-podem-causar-prejuizos-bilionarios-/21997/>.
- Farinnaccio, A., Goya, S., and Tessler., M. (2009). Variações da linha de costa nas baías de Santos e São Vicente. *Quaternary and Environmental Geosciences*, 01(1):42–48.
- Franz, G. A. S., Leitão, P., dos Santos, A., Juliano, M., and Neves, R. (2016). From regional to local scale modelling on the south-eastern Brazilian shelf: case study of Paranaguá estuarine system. *Brazilian Journal of Oceanography*, 64(3):277–294.
- FRF (2008). EIA-RIMA da dragagem de aprofundamento do canal de navegação, bacia de evolução e berços de atracação do Porto Organizado de Santos - São Paulo.
- Ganju, N. K., Brush, M. J., Rashleigh, B., Aretxabaleta, A. L., del Barrio, P., Grear, J. S., Harris, L. A., Lake, S. J., McCardell, G., O'Donnell, J., Ralston, D. K., Signell, R. P., Testa, J. M., and Vaudrey, J. M. P. (2016). Progress and challenges in coupled hydrodynamic-ecological estuarine modeling. *Estuaries and Coasts*, 39(2):311–332.
- Hamlington, B. D., Thompson, P., Hammond, W. C., Blewitt, G., and Ray, R. D. (2016). Assessing the impact of vertical land motion on twentieth century global mean sea level estimates. *Journal of Geophysical Research: Oceans*, 121(7):4980–4993.
- Harari, J. and Camargo, R. (1990). Estimation of the volume transport by the tides in the southeastern brazilian platform through a hydrodynamical model. In II Simpósio

- sobre ecossistemas da costa sul e sudeste brasileira: estrutura, função e manejo, *Águas de Lindóia*, 75–83.
- Harari, J. and Camargo, R. (1995). Tides and mean sea level variabilities in Santos (SP), 1944 to 1989. *Relatório Interno do Instituto Oceanográfico*, 36:1–15.
- Harari, J. and Camargo, R. (1998). Modelagem numérica da região costeira de Santos (SP): Circulação de maré. *Revista Brasileira de Oceanografia*. 46(2):135-156.
- Harari, J. and Camargo, R. (1999). Implantação de um sistema de previsão de marés e de correntes de maré na Baixada Santista através de modelo numérico tridimensional. *Relatório Técnico do Instituto Oceanográfico*. 45:1-21.
- Harari, J., Camargo, R., Augusto, C., França, D. S., Mesquita, A. R. D., and Picarelli, S. S. (2002). Modelagem numérica hidrodinâmica tridimensional da região costeira e estuarina de São Vicente e Santos (SP). *Pesquisa Naval - Suplemento Especial da Revista Marítima Brasileira*, 15:79–97.
- Harari, J., França, C., and Camargo, R. (2008). Climatology and hydrography of santos estuary. *Perspectives on Integrated Coastal Zone Management in South America*, IST PRESS,147-154.
- Harari, J. and Gordon, M. (2001). Simulações Numéricas da Dispersão de Substâncias no Porto e Baía de Santos, sob a Ação de Marés e Ventos. *Revista Brasileira de Recursos Hídricos*, 6(4):115–131.
- HIDROMOD (2016). *AQUASAFE Oil Spill Simulator User Manual*, 75.
- Horsburgh, K. J. and Wilson, C. (2007). Tide-surge interaction and its role in the distribution of surge residuals in the North Sea. *Journal of Geophysical Research: Oceans*, 112(8):1–13.
- Huthnance, J. M. (1980). On natural oscillations of connected ocean basins. *Geophysical Journal International*, 61(2):337–354.
- Kourafalou, V., De Mey, P., Staneva, J., Ayoub, N., Barth, A., Chao, Y., Cirano, M., Fiechter, J., Herzfeld, M., Kurapov, A., Moore, A., Oddo, P., Pullen, J., van der Westhuysen, A., and Weisberg, R. (2015). Coastal Ocean Forecasting: science foundation and user benefits, *Journal of Operational Oceanography*, 8:sup1, s147-s167.
- Leitão, J., Silva, A., and B, G., N. (2000). Estudo do melhor local para o descarte de lodos dragados no Porto de Santos. In *IX SILUBESA – Simpósio Luso-Brasileiro de Engenharia Sanitária e Ambiental*, Porto Seguro (BA), Brasil.

- Leitão, P. (2003). Integração de Escalas e Processos na Modelação do Ambiente Marinho. PhD Thesis, Universidade Técnica de Lisboa, 279.
- Leitão, P., Leitão, J., Neves, R., Berzin, G., and Silva, A. (2005). Hydrodynamics and transport in the coastal zone of São Paulo - Brazil. Conference proceedings, 14.
- Leitão, P., Leitão, J., Ribeiro, R., Sampaio, A., Galvão, P., Ribeiro, J., and Silva, A. (2015). Serviços de previsão de alta resolução de condições meteo-oceanográficas e de eventos de poluição costeira. VIII Congresso sobre Planeamento e Gestão das Zonas Costeiras dos Países de Expressão Portuguesa, 1–15.
- Lellouche, J. and Regnier, C. (2015). Global Ocean Sea Physical Analysis and Forecasting Products. Product User Manual, 16.
- Lopes, P. (2015). *As assimetrias de maré no Estuário de Santos, SP, Brasil*. PhD thesis, Universidade Federal Rio Janeiro.
- Lopes, P. G. (2015). *As assimetrias de Maré no Estuário de Santos - SP, Brasil*. PhD Thesis, Universidade Federal do Rio de Janeiro, 102.
- Mancuso, M., Ferreira, J. P., and Filho, J. L. (2014). Using GIS and modeling to assess groundwater discharge to Santos Estuary, Brazil. Technical report, 9.
- Martins, F., Neves, R., and Leitão, P. (1998). A three-dimensional hydrodynamic model with generic vertical coordinate. *Hydro-informatics*, 98:1403–1410.
- Mateus, M., Giordano, F., Marín, V. H., and Marcovecchio, J. (2008). Coastal zone management in South America with a look at three distinct estuarine systems. Perspectives on Integrated Coastal Zone Management in South America, IST PRESS, 43–58.
- Miranda, L. B., Olle, E. D., Bérghamo, A. L., Silva, L. D. S., and Andutta, F. P. (2012). Circulation and salt intrusion in the piaçaguera channel, Santos (SP). *Brazilian Journal of Oceanography*, 60(1):11–23.
- Moscatti, M., Pereira, C. S., Giarolla, E., and Santo, C. M. d. E. (2000). Estudo climatológico sobre a costa sul - sudeste do Brasil (Partes I, II e III). In Congresso Brasileiro de Meteorologia, 735–744.
- Moser, A., Giancesella, S. M., Cattena, C., David, C., Barrera-Alba, J., and Saldanha-Corrêa F M P, B. E. S. (2002). Aspectos da eutrofização na Baixada Santista: distribuição espaço temporal de biomassa fitoplanctônica e produtividade primária;

- transporte de nutrientes, material em suspensão e biomassa fitoplanctônica. In Anais do Congresso Brasileiro de Pesquisas Amb.
- Oliveira, M. D., Ebecken, N. F., Santos, I. D. A., Neves, C. F., Caloba, L. P., and de Oliveira, J. (2006). Modelagem da maré meteorológica utilizando redes neurais artificiais: uma aplicação para a Baía De Paranaguá – Pr , Parte 1: Dados meteorológicos da estação de superfície. *Revista Brasileira de Meteorologia*, 21(2):220–231.
- Pawlowicz, R., Beardsley, B., and Lentz, S. (2002). Classical tidal harmonic analysis including error estimates in MATLAB using T\_TIDE. *Computers and Geosciences*, 28(8):929–937.
- Pickard, S. and Pond, G. (1978). *Introductory Dynamical Oceanography*. Pergamon Press, Oxford, 349.
- Pugh, D. (1987). *Tides, Surges and Mean Sea-level*. Chichester (U.K), John Wiley & Sons, 472.
- Pugh, D. and Woodworth, P. (2014). *Sea-Level Science: Understanding Tides, Surges, Tsunamis and Mean Sea-Level Changes*. Cambridge University Press, 395.
- Riflet, G., Refray, G., Fernandes, R., Chambel, P., Nogueira, J., and Neves, R. (2010). Downscaling a large-scale ocean-basin model: An intercomparison exercise in the Bay of Biscay. In *V European Conference on Computational Fluid Dynamics*, 20.
- Santos, A. J. (1995). *Modelo hidrodinâmico tridimensional de circulação oceânica e estuarina*. PhD Thesis, Universidade Técnica de Lisboa, 273.
- Speranzini, B. T. (2017). *On physical oceanography of the Santos Estuary*. PhD Thesis, Delft University of Technology, 159.
- Taylor, K. E. (2001). Summarizing multiple aspects of model performance in a single diagram. *Journal of Geophysical Research: Atmospheres*, 106(D7):7183–7192.
- Tessler, M. G., Goya, C. Y., Yoshikawa, P., and Hurtado, S. N. (2006). *Erosão e progradação do litoral Brasileiro: São Paulo*. In *Erosão e progradação no litoral brasileiro*. Brasília: Ministério do Meio Ambiente, 297-346.
- Titarelli, A. (1986). *A Serra do Mar. Orientação - São Paulo*. Technical report. 7(86-93).
- Truccolo, E. C. (1998). *Maré meteorológica e forçantes atmosféricas locais em São Francisco do Sul- SC*. PhD Thesis, Universidade Federal de Santa Catarina, 100.

- Vaz, N. (2007). Study of heat and salt transport processes in the Espinheiro Channel (Ria de Aveiro). PhD Thesis, Universidade de Aveiro, 170.
- Vaz, N. and Dias, J. M. (2013). Physical analysis of a tidal channel (Espinheiro channel, Portugal): A modelling study. *Ocean modelling for coastal management - Case studies with MOHID*. IST PRESS, 41-54.
- Vaz, N., Dias, J. M., Leitão, P. C., and Nolasco, R. (2007). Application of the Mohid-2D model to a mesotidal temperate coastal lagoon. *Computers and Geosciences*, 33(9):1204–1209.
- Willmott, C. J. (1981). On the validation of model. *Physical Geography*, 2:219–232.